Minerals Engineering 249 (2026) 110835

Contents lists available at ScienceDirect

Minerals Engineering

journal homepage: www.elsevier.com/locate/mineng

Mitigating water quality deviations in recycled streams for concentration plants through the W-PIM/CP framework

Luis A. Cisternas [a,c,*], Israel Ponce-Lizarazu [a], Marinka Silva [a], Nathalie Jamett [b], Andrzej Kraslawski [d,e]

[a] Department of Mineral Process and Chemical Engineering, Universidad de Antofagasta, Antofagasta 1270300, Chile
[b] Sustainable Minerals Institute International Centre Chile (SMI Chile), The University of Queensland, Santiago, Chile
[c] Advanced Mining Technology Center (AMTC), Chile
[d] Department of Industrial Engineering and Management, LUT University, Lappeenranta, Finland
[e] Systems Research Institute, Polish Academy of Sciences, Warsaw, Poland

ARTICLE INFO

Keywords:
Property Integration
Water Optimization
Mineral Processing
Recycled Water
Pareto Frontier

ABSTRACT

Water scarcity and environmental regulations have increased water recycling in mining operations. However, traditional water management is based on mass balances and does not track changes in water quality in closed-loop systems. Recycled streams frequently accumulate physical and chemical impurities, such as multivalent ions and residual organics, and exhibit variations in physical properties, including dissolved oxygen and density, all of which can affect the kinetics and selectivity of mineral separation processes.

This study proposes a generalized framework for water management in mineral concentration plants using the Water Property Integration Method for Concentration Plants (W-PIM/CP). This approach utilizes surrogate properties, known as clusters, to track and optimize a vector of physical and chemical attributes. A mathematical programming model based on Mixed-Integer Nonlinear Programming (MINLP) was developed to address the nonlinearity inherent in property-mixing rules.

As a proof-of-concept application, the framework was illustrated on a sulfide flotation circuit using four water sources: fresh water, thickener water, tailings pond water, and thermal oxidation water. Ternary cluster diagrams provide an intuitive visualization for up to three properties, whereas the MINLP model is required to handle higher-dimensional property networks. A sensitivity analysis across a range of target property values for $SO4^{2-}$, Mg^{2+}, and dissolved oxygen showed that a segregated-water strategy consistently yields lower deviations from target pulp properties than a single process-water stream, at both the rougher and cleaner 1 stages. The reported freshwater figures therefore correspond to allocation among addition points within the circuit, not to a reduction of plant-wide make-up water, which is governed by the overall water balance and by physical losses such as evaporation and infiltration. The relevance of this allocation is metallurgical: blending fresh and recycled streams at specific addition points helps preserve the target water properties at each stage, whereas centralized commingling of all sources maximizes property deviations and was the least favorable configuration tested. These results support segregated, quality-driven water allocation in concentration plants. In addition, a Pareto analysis quantified the trade-off between freshwater consumption—progressively substituted with saltwater—and the resulting deviation from target pulp-property values at each flotation stage, showing that a segregated-water strategy can reduce freshwater use by up to 37 % relative to a single process-water pool at an equivalent deviation level.

1. Introduction

Water consumption in the mining industry is associated with critical issues affecting both environmental health and the long-term sustainability of operations. High water demand for processes such as ore processing, dust suppression, and equipment cooling places significant strain on local resources, particularly in arid and hyper-arid areas. This demand often competes with the needs of local communities and agriculture in regions with limited water availability, potentially leading

* Corresponding author.
E-mail address: luis.cisternas@uantof.cl (L.A. Cisternas).

https://doi.org/10.1016/j.mineng.2026.110835
Received 11 February 2026; Received in revised form 31 July 2026; Accepted 30 August 2026
Available online 4 September 2026

Nomenclature

$N_{sources}$	Number of streams
$M_{properties}$	Number of raw properties
N_{sinks}	Number of process units (Sinks)
N_{fresh}	Number of fresh water sources
N_{pulp}	Number of pulp flows
ψ_p	Property operator of property p
$p_{p,i}$	Value of the property p in stream i
$\overline{p}_p$	Mean property of the multicomponent mixture
x_i	Fractional contribution of the stream i
$\Omega_{p,i}$	Dimensionless operator of property p in stream i
ψ_p^{ref}	Property operator reference value
AUP_i	Augmented property index for each stream i
AUP_m	Mean stream augmented property index
AUP_{max}	Maximum limit of augmented property index
AUP_{min}	Minimum limit of augmented property index
$\overline{AUP}$	Resulting augmented property index
$C_{p,i}$	Cluster for property p in stream i
β_i	Cluster arm in stream i
$\overline{C}_p$	Mean cluster of N streams
F_r	Total freshwater flow in stream r, t/h
$f_{r,j}$	Individual freshwater flow$r$ towards process unit j, t/h
W_i	Total flow from each water source i, t/h
$w_{i,j}$	Individual flow from each water source$i$ toward any process unit (Sink) j, t/h
G_j	Total flow in process unit (Sink) j, t/h
m_j	Pulp flow toward process unit (Sink) j, t/h
$\psi_p\left(\overline{p}_{p,j}\right)$	Mean property operator from the final mixing of process unit (Sink)j
$\psi_p\left(p_{p,r}\right)$	Property operator p of freshwater flow r
$\psi_p\left(p_{p,i}\right)$	Property operator p of water source i
$\psi_p\left(p_{p,j}\right)$	Property operator p of process unit (Sink)j
BFR	Boundaries of the feasibility region
DO	Dissolved oxygen
DoE	Design of experiments
MINLP	Mixed-Integer Nonlinear Programming
NPV	Net present value
OPEX	Operating expenses
ORP	Oxidation-reduction potential
TOC	Total organic carbon
W-PIM/CP	Water Property Integration Method for Concentration Plants
2D	Two-dimensional graphic
3D	Three-dimensional graphic Indices
i	Process stream (Water source)
p	Property
r	Fresh water
j	Process unit (Sink)

to social conflicts and shortages (Lin et al., 2025). To mitigate these impacts and reduce operational costs, improving water efficiency and recycling is essential, although it requires substantial investment in technology and infrastructure (De Lima et al., 2025).

The challenges are further compounded by climate change and seasonal weather patterns, which exacerbate water scarcity, lead to unpredictable availability, and alter water quality (Corin et al., 2024). Furthermore, mining companies must adhere to increasingly stringent regulations on water usage and discharge to protect the environment. Excessive consumption can also jeopardize the social license to operate if it affects the local water supply. While mining accounts for only a small percentage of total water supply in some countries, e.g., 3 % in Chile, its regional impact is far greater in desert areas, where mining consumption can account for over 50 % of total water use (Ruffino et al., 2022). In these regions, water is a strategic and scarce resource, essential to concentration processes, where it typically accounts for 80–85 % of the volume of the mineral pulp processed in flotation circuits (Levay et al., 2001). Specifically in Chile, recycled water accounted for 75–76 % of the total (Cochilco, 2023). Some companies are turning to alternative water sources, such as seawater or treated wastewater, to lessen reliance on local supplies (Cisternas and Gálvez, 2018; Leiva González and Onederra, 2022).

Mineral concentration processes are highly dependent on water characteristics (Gao et al., 2021; Liu et al., 2013). For instance, pH levels are vital for reagent efficacy and process selectivity (Foroutan et al., 2021; Göktepe, 2002). Hard water, rich in calcium and magnesium ions, can hinder the action of flotation reagents, while high concentrations of dissolved solids or salinity can alter mineral surface properties performance (Cruz et al., 2022; Manono et al., 2012). Impurities such as iron, sulfur, and organic compounds can adversely affect performance by coating mineral surfaces and inhibiting bubble attachment (Sinche-Gonzalez et al., 2016). Furthermore, the oxidation state of minerals and their floatability are influenced by temperature (Bicak et al., 2023) and the water's oxygen content (Zhang et al., 2025b). Specific metal ions play direct and indirect roles in mineral separation. Research has shown that high calcium concentrations can suppress sulfide minerals such as chalcopyrite by interfering with the adsorption of xanthate collectors (Liu and Zhang, 2000; October et al., 2020). Similarly, increasing magnesium ion concentrations can diminish recovery by forming hydrophilic precipitates on mineral surfaces (Hirajima et al., 2016). When lime is used as a pH modifier, the presence of sulfate ions can trigger the precipitation of calcium sulfate, forming thin layers that hinder flotation and reduce selectivity (Grano et al., 1997; Lucay et al., 2015; Raghavan and Hsu, 1984; Sinche-Gonzalez and Fornasiero, 2021; Zanin et al., 2019). Conversely, certain ions, such as copper, can activate mineral surfaces under specific conditions, thereby improving hydrophobicity. The impact of other ions in seawater is discussed in the literature (Gálvez et al., 2014; Jeldres et al., 2016).

While water recycling and reuse help conserve resources, they also tend to concentrate dissolved and suspended impurities in the circuit over time (Levay et al., 2001), which can degrade water quality and reduce flotation performance. To offset this performance loss, some operations incorporate fresh water into the flotation circuit even when high overall recycling rates are pursued for environmental and regulatory reasons (Aaltonen et al., 2023; Soufiabadi et al., 2024). In such cases, fresh water is not added solely to compensate for physical losses such as evaporation, infiltration, and entrainment in tailings; it also serves as a metallurgical input that helps maintain the water-quality conditions required for recovery and selectivity. Several studies have examined how different water sources should be combined to preserve flotation performance: for example, El-Bacha et al. (2025) reported that a 50/50 blend of fresh and recycled water yielded approximately 80 % copper recovery at the Bleida Mine (Morocco), while the use of recycled water alone resulted in markedly lower recoveries. Despite this evidence, many mining operations currently combine different water sources without a quantitative understanding of how these mixtures affect overall pulp properties. This lack of integrated management makes it difficult to attribute changes in recovery or product quality to specific water-quality drivers.

The objective of this study is to propose a generalized framework, W-

PIM/CP, that incorporates water quality into the management of mineral concentration plants through the property integration method. The approach uses property operators and property clusters to track and match physical and chemical attributes across the water network, and to support the allocation and blending of available water sources, including recycled streams and fresh water as make-up water. In this framework, fresh water is treated not only as a hydrological input but also as a means of adjusting water-quality conditions at flotation addition points. The framework is illustrated on a sulfide concentration circuit through a Mixed-Integer Nonlinear Programming (MINLP) model that minimizes the difference between calculated and desired property operators at the selected addition points respecting the target property windows of each flotation stage.

Compared with conventional water management in mineral processing, which is based primarily on volumetric balances, the contribution of this work is threefold. First, the framework allows the simultaneous management of multiple non-conservative water-quality variables, including dissolved oxygen (DO), pH, conductivity, and several ionic species (Mg^{2+}, Ca^{2+}, SO_4^{2-}), within a single optimization model. Second, it adapts the property-cluster representation to flotation operations, enabling a graphical mapping of feasible operating regions in ternary diagrams as a complement to the algebraic model. Third, it formulates the choice between allocating segregated water and process water by analyzing deviation from target pulp properties as a multi-objective problem, producing designs that make the trade-off explicit. These elements are presented as a proof of concept; their industrial use would require site-specific calibration, as discussed in Section 3.5.

This manuscript is organized as follows: Section 2 details the proposed methodology and the development of the MINLP optimization model. Section 3 presents the practical application of the methodology, demonstrating how to manage multiple water sources and generate Pareto-optimal designs. Section 4 concludes the study and outlines future work to standardize mining operations within this integrated property framework.

2. Methodology

The methodology proposed in this work, designated as the Water Property Integration Method for Concentration Plants (W-PIM/CP), is a holistic framework that optimizes water utilization by integrating physical and chemical properties with traditional mass balances. The W-PIM/CP follows a structured workflow that transitions from empirical data collection to advanced mathematical optimization (see Fig. 1).

The proposed methodology is analyzed in a case study that outlines its practical application. These methodologies encompass several key steps or modules. The first one, physical domains and characterization, begins with an analysis of the plant configuration. This initial phase is critical for understanding water management, locating additional points, and identifying water sources. Also, the baseline flow rates are established, and the "vector" of properties is defined. Following this, the methodology involves collecting samples and data, providing the necessary empirical foundation for the subsequent stages.

The next step is to implement property integration calculations. This phase is at the core of the methodologies, in which the collected data is analyzed and interpreted using the principles of property integration. This process is crucial for identifying and understanding the factors that influence water use in mining. Also, ternary diagrams are used as an initial visualization of the problem.

In module 3, the mass and property balance equations are used to develop a Mixed-Integer Non-Linear Programming (MINLP) model, including the selection of objective functions, e.g., minimizing the difference between calculated and desired property operators for meeting target property values to achieve optimal mineral recovery.

Finally, in Decision Domain & Selection, a comprehensive analysis is

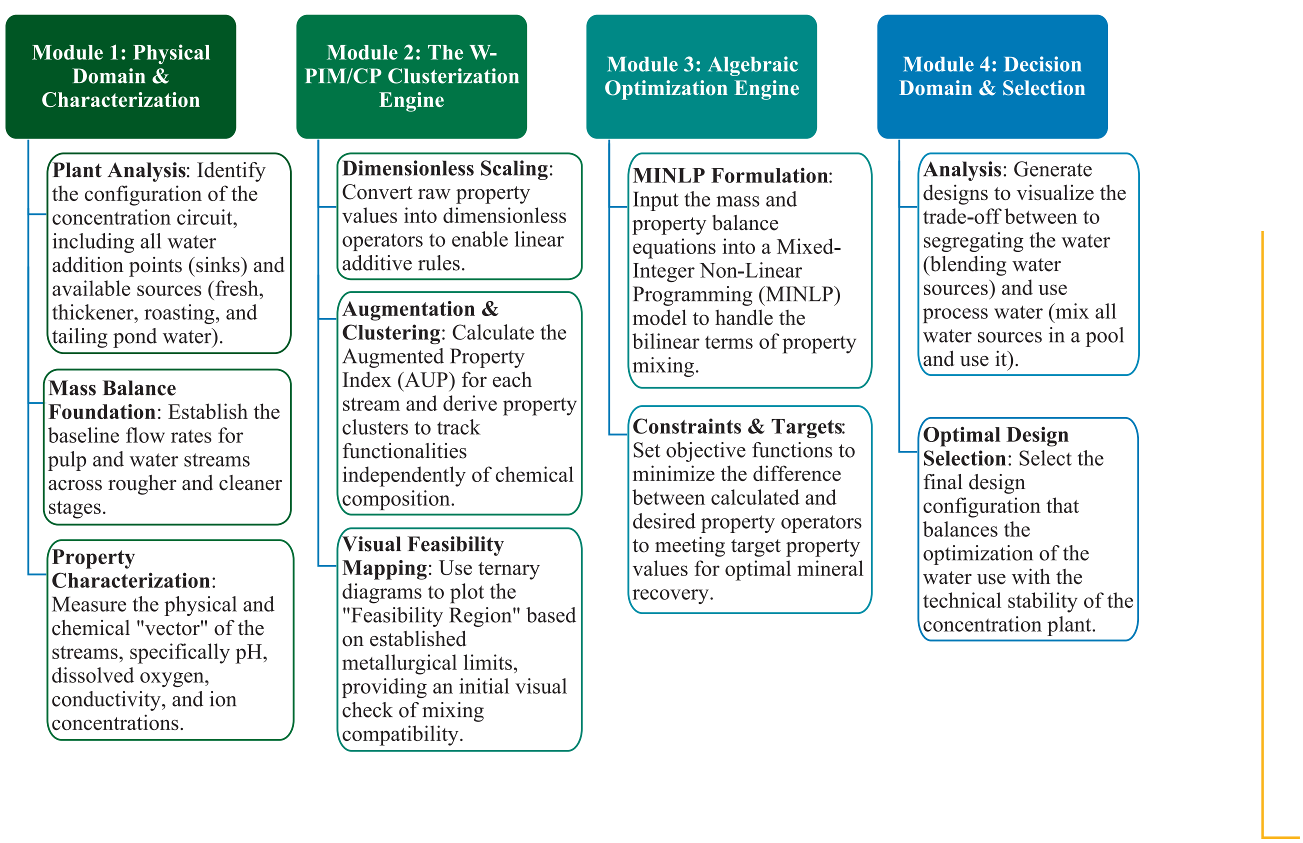

Fig. 1. The W-PIM/CP (Water Property Integration Method for Concentration Plants) framework. A multi-stage approach transitioning from physical stream characterization and property clusterization to MINLP optimization.

done based on designs to visualize the trade-off between sustainability and operational precision. This stage not only highlights the outcomes of the calculations but also provides insights, recommendations based on the findings, and a comparison between alternatives. The analysis aims to provide actionable solutions or strategies to optimize water management in the mining industry, thereby enhancing both environmental sustainability and operational efficiency.

2.1. Case study definition and analysis of the plant configuration

The studied process corresponds to a concentration plant in the Antofagasta region of Chile that processes copper ore. The typical mineralogy of this ore includes valuable species such as chalcopyrite, bornite, enargite, chalcocite, and covellite, while pyrite is the main sulfurous gangue. The non-sulfurous gangue is mainly composed of feldspars, silica, and some clay species like muscovite, kaolinite, paragonite, phengite, and illite. The main stages of the plant are grinding, rougher flotation, regrinding, and cleaning flotation (See Fig. 2). The rougher flotation circuit consists of a rougher stage that receives the pulp from the grinding stage and is mixed with water to achieve a lower percentage of feed solids. The tailings from the rougher stage are sent to the final tailings stream, and the concentrate from this stage is sent to the cleaning stage.

The cleaning circuit consists of 4 stages: 1st Cleaning, 2nd Cleaning, 1st Scavenger, and 2nd Scavenger. The main water mixing points correspond to the rougher feed and the first cleaning feed. Water recovered from the thickening process, the tailing pond, and the thermal oxidation process is collected in a process water pool and sent to the required stages (see Fig. 2).

As shown in Fig. 2, water is added at the entrance to the rougher flotation stage and at the entrance of the 1st Cleaning stage to maintain the solid percentage at desired levels. Before presenting the stagewise balance, it is useful to situate the flotation circuit within the broader water network of the plant. The balance reported in Table 1 covers the flotation circuit between the grinding discharge and the final concentrate and tailings streams; it does not explicitly quantify the physical water losses that govern plant-wide make-up requirements. In a typical sulfide concentrator, these losses occur in units located downstream of the flotation circuit and follow four main pathways: (i) water retained as moisture in the deposited tailings at the tailings storage facility, which is generally the largest individual loss; (ii) evaporation from the tailings storage facility and from open process-water pools, particularly relevant under the arid conditions of northern Chile; (iii) infiltration and seepage at the tailings storage facility; and (iv) moisture in the final concentrate leaving the filter. These losses are compensated by freshwater make-up entering the process-water pool (Fig. 2). The W-PIM/CP framework operates on the allocation of the available water sources among internal addition points and does not modify these physical losses, which depend on tailings dewatering technology, climatic conditions, and the design of the tailings storage facility. Table 1 therefore presents the internal mass balance of the flotation circuit, while the recycling and make-up streams that close the broader water network are represented in Fig. 2.

2.2. Sample and data collection

Once the water addition points have been identified and their flow rates characterized, it is necessary to assess their impact on the plant's operation and performance. In this case study, the most important properties are those that affect copper recovery at each flotation stage.

The literature suggests that the properties of the water used in the concentrator plant can influence performance in various ways and to varying degrees, depending on the point of addition. Table 2 summarizes the literature, highlighting the principal effects of these properties on copper recovery. Although additional effects on copper recovery are documented in the literature, the properties selected for this case study were chosen for their relevance. Determining the most suitable property values for operation is important; however, it is beyond the scope of this paper. A discussion on this point is included below, in the future work subsection.

To characterize the streams, samples were collected at the water addition point, as depicted in Fig. 2. Two types of samples were collected. The first type is processed pulp, a mixture of water and copper-containing ore with specified solids content. The second type of sample corresponds to the water added to adjust the solids percentage. The quality of this water varies depending on whether it is fresh water or recycled water from mining operations.

For all samples, sulfate (SO_4^{2-}) concentration was quantified by gravimetry, and copper (Cu^{2+}), magnesium (Mg^{2+}), and calcium (Ca^{2+})

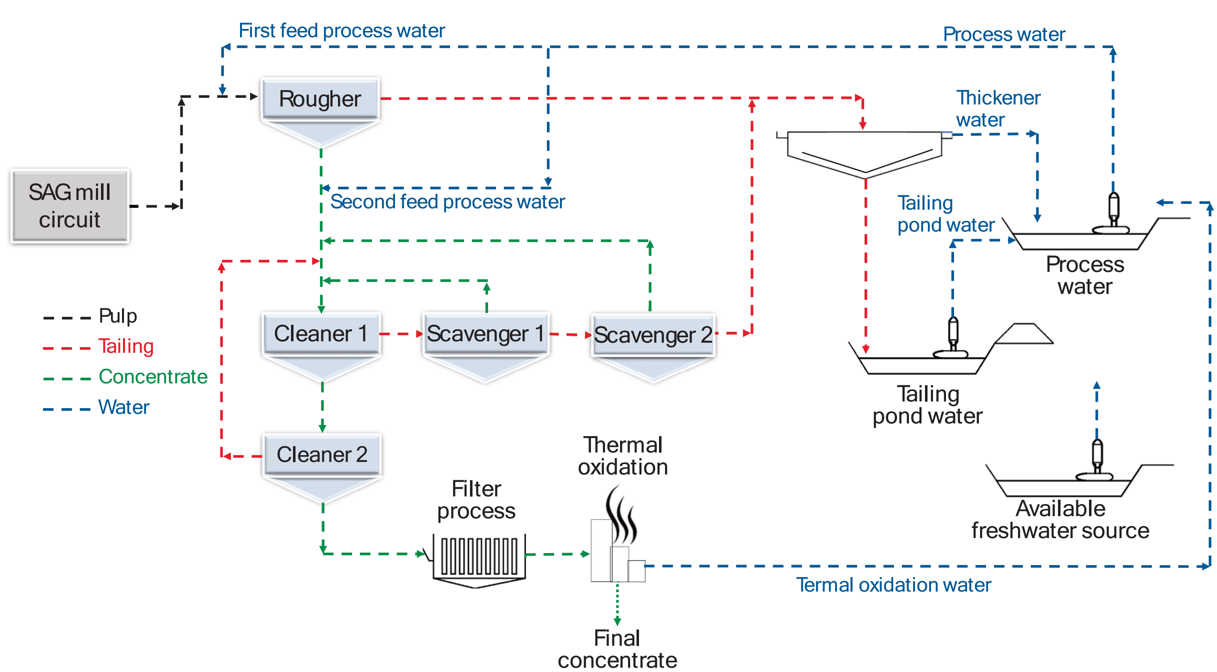

Fig. 2. Flotation circuit of chalcopyrite with recycled process water distribution.

Table 1
Pulp and water mass flow rates used in the flotation circuit case study.

Stream	Units	Flotation stage Rougher	Cleaner 1	Cleaner 2	1st Scavenger	2nd Scavenger
Pulp feed	t/h	9143	5176	1846	4325	3812
Water feed	t/h	1524	995	0	0	0
Pulp concentrate	t/h	2978	1846	644	513	482
Pulp tail	t/h	7689	4325	1202	3812	3330

Notes: 1) For this table, internal pulp recirculation flows were omitted.
2) All flows are either pulp or water.

concentrations were measured using atomic absorption spectrometry. Dissolved oxygen (DO) was determined based on Standard Methods for the Examination of Water and Wastewater. Chemical properties such as pH, redox potential (ORP), and conductivity were also determined by Hanna multi-parameter meter, model HI98194. Table 3 presents the characterization of the samples described.

2.3. Property integration calculations

The main objective of process integration is to holistically design and optimize entire chemical and metallurgical systems, not just individual units, to maximize efficiency, minimize costs, reduce resource use (energy, water, materials), and lower environmental impact. By exploiting synergies and interactions, process integration aims to reduce investment and operating costs, increase yields, and achieve a more sustainable footprint through techniques such as energy recovery (heat integration) and water reuse (mass integration), thereby contributing to greener processes. Property Integration is a method for incorporating properties into traditional heat and mass integration methodologies (El-Halwagi, 2017). Therefore, property integration is a holistic, functionality-based approach to allocating and manipulating streams and processing units, grounded in functional properties throughout the process, including mass and energy integration. It is based on tracking, adjusting, assigning, and matching functionalities throughout the process (El-Halwagi et al., 2004) Many of these processing units are designed to accept streams with specific property ranges, regardless of their chemical composition. Generally, these properties are measured in different units, making it challenging to base design decisions on key properties. To overcome this situation, the Property Integration Methodology employs surrogate properties, known as 'clusters,' to conserve property measurements during mixing operations. The basic mathematical expressions for cluster calculation are given by Shelley and El-Halwagi, (2000).

2.4. Property integration calculations

The main objective of process integration is to holistically design and optimize entire chemical and metallurgical systems, not just individual units, to maximize efficiency, minimize costs, reduce resource use (energy, water, materials), and lower environmental impact. By exploiting synergies and interactions, process integration aims to reduce investment and operating costs, increase yields, and achieve a more sustainable footprint through techniques such as energy recovery (heat integration) and water reuse (mass integration), thereby contributing to greener processes. Property Integration is a method for incorporating properties into traditional heat and mass integration methodologies (El-Halwagi, 2017). Therefore, property integration is a holistic, functionality-based approach to allocating and manipulating streams and processing units, grounded in functional properties throughout the process, including mass and energy integration. It is based on tracking, adjusting, assigning, and matching functionalities throughout the process (El-Halwagi et al., 2004). Many of these processing units are designed to accept streams with specific property ranges, regardless of their chemical composition. Generally, these properties are measured in different units, making it challenging to base design decisions on key properties. To overcome this situation, the Property Integration Methodology employs surrogate properties, known as 'clusters,' to conserve property measurements during mixing operations. The basic mathematical expressions for cluster calculation are given by Shelley and El-Halwagi, (2000).

Suppose that we have N streams or sources. Each stream is characterized by M raw properties. Consider the class of properties whose mixing rules for each raw property are given by the following equation:

$$\psi_p\left(\bar{p}_p\right) = \sum_{i=1}^{N_{sources}} x_i \psi_p\left(p_{p,i}\right) \tag{1}$$

where x_i is the fractional contribution of the i^{th} stream into the total flow rate of the mixture and $\psi_p\left(p_{p,i}\right)$ is an operator of the property on the stream $(p_{p,i})$ which can be normalized into a dimensionless operator by dividing by a reference value.

$$\Omega_{p,i} = \frac{\psi_p(p,i)}{\psi_p^{ref}} \tag{2}$$

The operator $\Omega_{p,i}$ can be evaluated from first principles or estimated through empirical or semi-empirical methods aiming the formulation of linear mixing rules, see Equation (1). Examples of property operator expressions can be found in the literature (Kazantzi, 2006; Li et al., 2022; Sandate-Trejo et al., 2014; Shelley and El-Halwagi, 2000).

Then, an augmented property index (AUP) for each stream i is defined as the summation of the dimensionless raw property operators:

$$AUP_i = \sum_{p=1}^{M_{properties}} \Omega_{p,i} \tag{3}$$

The cluster for property p in stream i, $C_{p,i}$, is defined as follows

$$C_{p,i} = \frac{\Omega_{p,i}}{AUP_i} \tag{4}$$

Therefore, one can show intra-stream conservation for clusters. In other words, for any stream i, the sum of clusters must be conserved adding up to a constant (for example, unity), that is

$$\sum_{p=1}^{N_c} C_{p,i} = 1 \tag{5}$$

Let the cluster arm be defined as

$$\beta_i = \frac{x_i AUP_i}{\overline{AUP}} \tag{6}$$

Where

$$\overline{AUP} = \sum_{i=1}^{N_{sources}} x_i AUP_i \tag{7}$$

Therefore, one can show inter-stream conservation upon mixing, which implies that

Table 2
Main effects of pulp properties on chalcopyrite and pyrite flotation recovery.

Property	Effect on chalcopyrite	Effect on pyrite	Reference
SO_4^{2-} [Concentration]	High concentrations of sulfate ions (SO_4^{2-}) and calcium ions (Ca^{2+}) show a depression of chalcopyrite due to the formation of a hydrophilic species on the surface. These hydrophilic species could be thiosulfates or sulfates.	Pyrite depression is caused by lime in flotation due to the formation of hydrophilic products like $CaOH^+$, $Ca(OH)_2$, $CaSO_4$, and $Fe(OH)_3$ on the pyrite surface.	(Castellón et al., 2022; Mu et al., 2016; Shen et al., 2001)
Dissolved oxygen (DO)	Moderate dissolved oxygen levels facilitate the electrochemical reactions that render the collector hydrophobic and enable it to adhere to the mineral surface. Excessive oxidation changes the chalcopyrite's hydrophobic surface into a hydrophilic one.	High dissolved oxygen levels oxidize the pyrite surface, forming hydrophilic species ($Fe(OH)_3$ or FeOOH) that prevent collector attachment.	(Fan et al., 2025; Kuopanportti et al., 1997)
Cu^{+2} [Concentration]	The copper ions can increase the flotation rate under certain conditions. Copper ions in the form of hydrolyzed species (Cu(OH) and $Cu(OH)_2$) can absorb onto the chalcopyrite surface.	The presence of copper ions in the pulp activates pyrite.	(Gao et al., 2021; Sun et al., 2023; Zhang et al., 2020)
	Cu^{2+} exchange electrons with sulfur on the chalcopyrite surface, thereby improving its hydrophobicity.		(Zhang et al., 2025a)
Ca^{2+} and Mg^{2+} [concentration]	Products formed by Ca^{2+} (e.g., $Ca(OH)^+$, $Ca(OH)_2$) at high pH values can absorb onto the chalcopyrite surface and reduce the recovery.	Ca^{2+} contributes to the depression of the pyrite, given that form compounds like $Ca(OH)_2$ or $CaSO_4$, which absorb onto the pyrite surface, forming a hydrophilic layer.	(Uribe et al., 2017)
	Mg^{2+} is considered a more potent depressant than Ca^{2+} in higher pH levels. The Mg^{2+} forms the $Mg(OH)_2$, and this precipitates on both chalcopyrite and pyrite surfaces. This layer is hydrophilic and blocks the collector.		(Gao et al., 2021)
Conductivity	Conductivity has a positive effect on copper recovery in the range from 0 to 12 mS/cm.		(Dzingai et al., 2020)
	High conductivity enhances the oxidation and dissolution of chalcopyrite by releasing copper ions, which activate pyrite and cause it to float.		(Mu and Peng, 2019; Owusu et al., 2014)
pH	Chalcopyrite maintains its floatability over a wider pH range than pyrite. The chalcopyrite surface has the ability to remain hydrophobic, to adsorb the collector, and maintain high recovery.	As the pH is increased into the alkaline range, promoting the oxidation and hydrolysis of the pyrite surface. A hydrophilic layer of ferric hydroxide, $Fe(OH)_3$, is formed on the pyrite surface. Pyrite recovery typically decreases sharply as pH rises above 9 and is minimized around pH 11–12.	(Castellón et al., 2022; Chi et al., 2020; Feng et al., 2024; Rios et al., 2025; Yang et al., 2025)

$$\overline{C}_p = \sum_{i=1}^{N_{sources}} \beta_i C_{p,i} \tag{8}$$

where $\overline{C}_p$ is the mean cluster resulting from adding the individual clusters of N streams.

Equations (1)–(8) define the property-cluster representation used in the W-PIM/CP framework. The dimensionless operators map raw, non-conservative properties onto a common basis on which mixing can be tracked as a linear combination of cluster arms (Eq. (8). This linear form is used in two ways in the remainder of the paper: a graphical assessment of stream compatibility through ternary diagrams (Section 3.1) and the algebraic formulation of the MINLP optimization model (Section 2.4).

It is important to clarify that the linear mixing rules used in the property-cluster formulation are methodological surrogates. In real sulfide flotation systems, linearity is not a general rule, since the response to water quality may be nonlinear and matrix-dependent due to pH-dependent speciation, mineral dissolution, redox reactions, precipitation, galvanic interactions, and residual reagents. Therefore, the property operators and feasible regions could provide a practical basis for water-allocation analysis, but their application should be supported by site-specific calibration using experimental data, plant surveys, or historical metallurgical performance.

In a process with specific sources (streams) and sinks (units or processes), along with their properties and constraints, graphical techniques were developed to identify optimal allocation and interception strategies. These techniques integrate the properties of sources, sinks, and interceptors to optimize a desirable process objective (e.g., minimum usage of fresh resources, maximum utilization of process resources, minimum cost of external streams), while satisfying the constraints on properties and flow rate for the sinks (El-Halwagi et al., 2004). This graphical technique utilizes three properties represented in ternary diagrams. The core of this visualization technique lies in accurately mapping the feasible property region. Using equations (1) to (8), it determines the optimal management of the mixing streams. The constraints on properties lead to the construction of the boundaries of the feasibility region (BFR), as detailed in El-Halwagi, (2017). This region is represented by six points, joined by linear segments derived from

Table 3
Properties characterization of flow samples of pulp and water used in the proposed methodology.

	SO_4^{2-} (mg/L)	DO (mg/L)	Cu^{2+} (mg/L)	Mg^{2+} (mg/L)	Ca^{2+} (mg/L)	Conductivity (µS/cm)	pH
Pulp							
Rougher Feed	1948	7.92	0.16	12.0	450	3705	8.9
Rougher concentrate	911	5.99	0.17	13.4	300	5554	8.6
Rougher tail	1014	1.24	0.13	0.3	373	7630	8.9
Cleaner 1 concentrate	1487	4.61	0.52	0.3	466	6720	11.9
Scavenger 2 tail	1115	0.52	0.13	0.4	194	7060	11.9
Scavenger 1 concentrate	957	0.97	0.18	0.4	216	7151	11.9
Scavenger 2 concentrate	1816	5.72	0.20	13.5	469	5176	12.0
Final concentrate	957	0.97	0.09	0.4	147	6045	12.0
Cleaner 2 tail	1204	2.10	0.15	0.3	226	7230	12.0
Water							
Process water	1805	5.89	0.16	2.4	632	5528	6.4
Thermal oxidation water	1720	8.20	0.73	22.0	120	4770	4.6
Thickener water	1600	6.89	0.14	1.3	629	5140	10.10
Fresh water	200	7.00	0.03	2.4	23	1036	8.0
Tailing pond water	2680	1.15	0.10	2.2	766	7320	3.5

the BFR's three convex hulls. The BFR represents the region containing the maximum and minimum properties allowed in the process. To briefly explain the calculation steps, consider the following illustrative example.

The first step in the methodology is to define the feasible region. This region is defined by the lower and upper limits of all considered inlet pulp properties, within which copper recovery is maximized. Based on the literature reviewed, Table 4 displays the property levels employed in this case study.

The property clusters are defined to exhibit intra- and inter-stream conservation patterns, thereby enabling the implementation of linear additive rules and their representation in ternary diagrams, called property cluster diagrams.

In order to ensure the feasibility of the mixture of streams into a process, the following conditions must be satisfied, according to the methodology from El-Halwagi (El-Halwagi, 2017).

The cluster value for the source (or mixture of sources) must be contained within the feasibility region of the cluster ternary diagram.
The values of the augmented property index for the mixture of sources and the process must match.
The flow rate of the source (or mixture of sources) must lie within the acceptable feed flow rate range for the process.

Conductivity (Cond), dissolved oxygen (DO), and sulfate (SO_4^{2-}) are the properties used in analysis on the ternary diagram. To determine the boundaries of the feasible region, the following combination of the maximum and minimum values of the dimensionless operator for each property is used: $(\Omega_C^{min}, \Omega_{DO}^{max}, \Omega_{SO4}^{max})$ $(\Omega_C^{min}, \Omega_{DO}^{min}, \Omega_{SO4}^{max})$ $(\Omega_C^{max}, \Omega_{DO}^{min}, \Omega_{SO4}^{max})$ $(\Omega_C^{min}, \Omega_{DO}^{min}, \Omega_{SO4}^{max})$ $(\Omega_C^{max}, \Omega_{DO}^{min}, \Omega_{SO4}^{min})$ $(\Omega_C^{max}, \Omega_{DO}^{min}, \Omega_{SO4}^{max})$.

By applying the property levels from Table 3 and using equations (1) to (5), it is possible to transform these coordinates into clusters. These clusters can then be plotted on the ternary diagram, thereby defining the boundaries of the feasible region.

Moving forward with the methodology, considering the first water addition point at the entrance of the rougher flotation circuit, the characterization of the streams indicates that they are combined in a pulp/water ratio of 4. Depending on the data collection method, several water quality parameters can be used, as shown in Table 3. For each stream, both the pulp and added water, it is possible to calculate their respective clusters using Equations (1) to (5). Additionally, Equations (6) to (8) can be employed to determine the new cluster resulting from the mixing of the two streams. Fig. 3a illustrates the construction of the feasible region, the clusters from the inlet streams, and the resulting point from the mixing of the pulp and thickener water.

On the other hand, Fig. 3b presents the AUP values for each stream and their combination. The maximum and minimum values are determined by calculating the AUPs within the feasible region. The AUP value for the rougher inlet pulp does not fall within the required AUP range, even though the AUP for the thickener water does. Mixing the two streams at the specified ratio yields a new AUP value that does not meet the required level. This new AUP from mixing can be calculated from Equation (7). It is important to note that, in this example, the condition is not met, underscoring an opportunity to improve water management. This could involve substituting the water source with a higher-quality source or adjusting the mixing ratios to achieve the desired quality, thereby meeting all three conditions specified in the methodology.

It is important to note that the property limits used in this study (Tables 4 and 6) serve to demonstrate the framework's mathematical mechanics. In practice, these targets must be defined through site-specific experimental protocols, such as a design of experiments (DoE), to ensure the 'Feasible Region' reflects the unique mineralogical and chemical matrix of the operation.

Table 4
Lower and upper levels of every property where copper recovery is maximized.

Property	Units	Min	Max
Conductivity	µS/cm	2000	6000
Dissolved Oxygen	mg/L	2	8
Mg^{2+}	mg/L	4	10
Ca^{2+}	mg/L	100	300
Cu^{2+}	mg/L	0.05	0.3
SO_4^{2-}	mg/L	600	2000

2.5. Optimization of mass and property integration

Unlike the graphical methodology of Section 2.3, which is restricted to three properties at a time, the algebraic formulation presented here handles multiple properties and multiple water sources simultaneously. The mixing-point balances contain bilinear terms in flow and property variables, so the resulting model is formulated as a Mixed-Integer Nonlinear Program (MINLP).

This mass and properties integration methodology aims to optimize the recycling and reuse of water in a given system achieving optimal properties in process units (sinks) (Nápoles-Rivera et al., 2010) using property operators. In this way, mineral recoveries and water management are improved simultaneously. The optimization structure of the methodology follows mainly the structure of Fig. 4. The scheme shows the feeding of N water sources with interesting properties; these water sources must be mixed at the arrival point or in the process units (sinks)

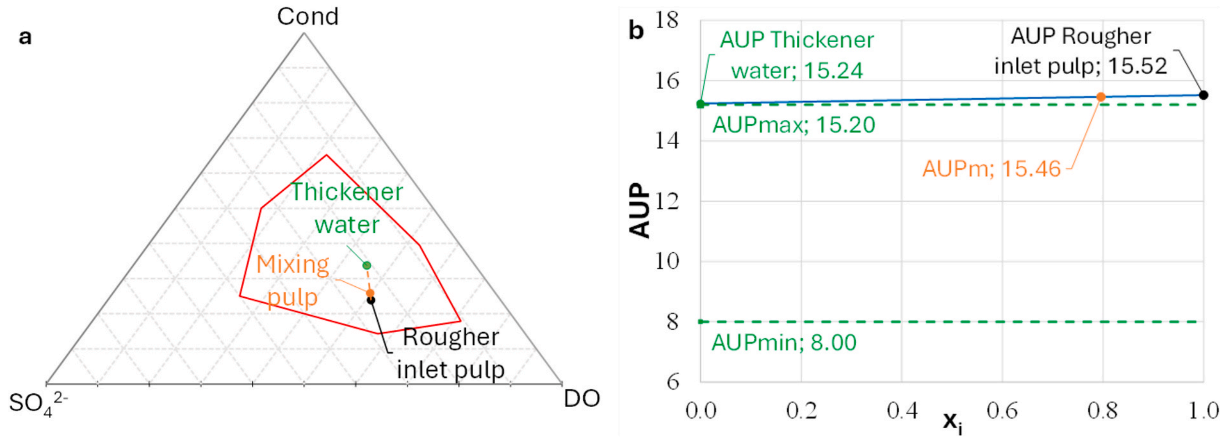

Fig. 3. (a) Ternary diagram of SO_4^{2-}, Cond, and DO showing feasible region and location of mixing pulp stream for the rougher circuit. (b) Location of mixing stream augmented property index (AUPm) value in a chart of augmented property index (AUP) required range.

Table 5
Property operators' values for every analyzed property.

Property	Operator	Reference
Concentration	$\psi_{Conc}(p_{Conc}) = [Concentration]$	(Deng et al., 2016; Jiménez-Gutiérrez et al., 2014; Zhang et al., 2021)
Conductivity	$\psi_{Cond}(p_{Cond}) = [Conductivity]$	This work
Dissolved Oxygen	$\psi_{OD}(p_{OD}) = [Oxygendemand]$	(Deng et al., 2016; Ding et al., 2020; Jiménez-Gutiérrez et al., 2014)
pH	If pH < 7 $=>$ $\psi_{pH}\left(P_{pH}\right) = 10^{-pH}$ If pH > 7 $=>$ $\psi_{pH}\left(P_{pH}\right) = 10^{pH-14}$	(Chen et al., 2010; Ding et al., 2020; Ng et al., 2008) (Chen et al., 2010)

Table 6
Desired property values in the rougher and cleaner 1 stage of the case study.

Property	Units	Rougher	Cleaner 1
Conductivity	µS/cm	4000	4000
Dissolved Oxygen	mg/L	8	3
Mg^{2+}	mg/L	7	6
Ca^{2+}	mg/L	200	300
Cu^{2+}	mg/L	0.25	0.15
SO_4^{2-}	mg/L	1000	1500
pH		8.0	11.5

with pulp streams that require water. The sinks (mix of water and pulp) must meet the optimal operational requirements.

When the methodology is applied, as shown in Fig. 4, it will achieve the ideal water feed mix (from various sources) to add to the pulp stream, ensuring optimal properties.

The following lines describe the mass and properties balance equations at the mixing points and the splitting of streams, along with the final mixing restraints (Nápoles-Rivera et al., 2010).

Splitting of freshwater sources:

$$F_r = \sum_{j=1}^{Nsinks} f_{r,j} \tag{9}$$

Where; F_r total freshwater flow, $f_{r,j}$ individual freshwater flow towards process unit (Sink).

Splitting of water sources:

$$W_i = \sum_{j=1}^{Nsinks} w_{i,j} \tag{10}$$

Where; W_i total flow from each water source, $w_{i,j}$ individual flow from each water source toward any process unit (Sink).

Mass balance in the mixing point before the entrance to the process units (Sinks)

$$G_j = \sum_{r=1}^{Nfresh} f_{r,j} + \sum_{i=1}^{Nsources} w_{i,j} + m_j \tag{11}$$

Where; G_j total flow or process unit (Sink), m_j pulp flow toward process unit (Sink).

Property tracking at the mixing point before the entrance to the process units (Sinks):

$$G_j{}^*\left[\psi_p\left(\overline{p}_{p,j}\right)\right] = \sum_{r=1}^{Nfresh} f_{r,j}{}^*\left[\psi_p\left(p_{p,r}\right)\right] + \sum_{i=1}^{Nsources} w_{i,j}{}^*\left[\psi_p\left(p_{p,i}\right)\right] + m_j{}^*\left[\psi_p\left(p_{p,j}\right)\right] \tag{12}$$

Where; $\psi_p\left(\overline{p}_{p,j}\right), \psi_p\left(p_{p,r}\right), \psi_p\left(p_{p,i}\right) y \psi_p\left(p_{p,j}\right)$ are mean property operators from the final mixing, the freshwater source, the process water source, and the pulp source respectively.

Table 5 describes the property operator values for concentration, dissolved oxygen, pH, and conductivity. The conductivity operator is considered equal to the conductivity, given the linearity of conductivity with respect to the ionic force of the water sources when the ion matrix is similar across the system under study. This consideration only applies to this case study.

According to Table 5, the property values are defined by their source of water or pulp, for example, in water sources stream the values of two properties are:

$$p_{Conc,1} = [Concentration] = \psi_{Conc}\left(p_{Conc,1}\right) \tag{13}$$

$$p_{pH,1} = 10^{pH-14} = \psi_{pH}\left(p_{pH,1}\right)[\text{If pH} > 7] \tag{14}$$

Equation (13) shows the concentration of the property in water source 1. Equation (14) shows the pH value of water source 1. This criterion applies to all water sources and pulp.

Property constraints in process units (Sinks) used to calculate the constraint property operators $\left(\psi_{p,j}\big|_{constraintvalue}\right)$*:*

$$p_{p,j}\Big|_{sinks} = p_{p,j}\Big|_{table6(constraintvalue)} \tag{15}$$

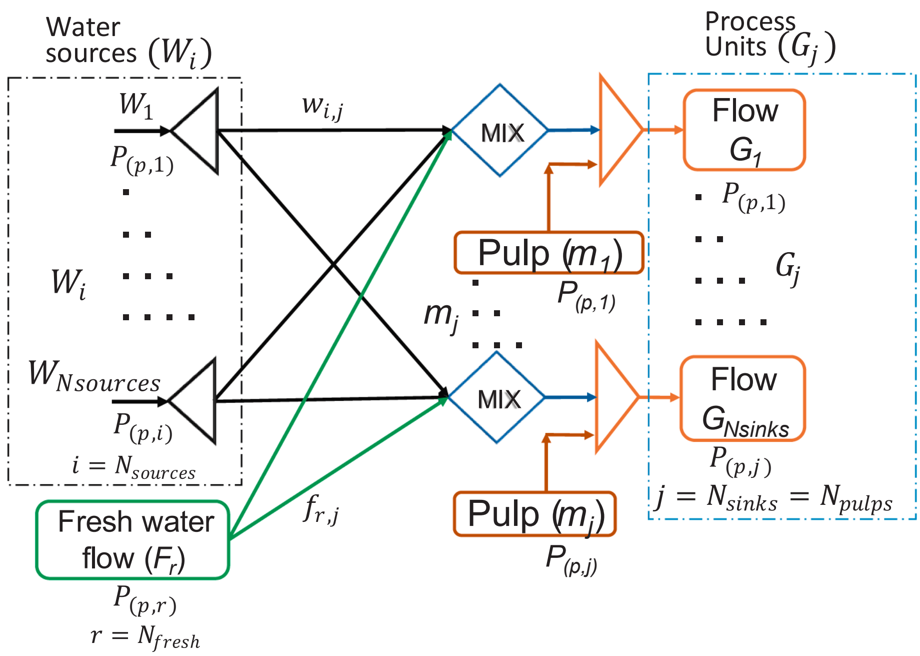

Fig. 4. Mass and property integration network scheme for fresh water, water sources (recycle water), pulp and process units, focusing on the reuse of water.

Constraints on freshwater consumption:

$$F_r = \sum_{j=1}^{Nsinks} f_{rj} = F_r|_{maxflow} \tag{16}$$

Objective function:

$$Min = \frac{\left(\psi_p\left(\bar{p}_{pj}\right)^{calculated} - \psi_p\left(\bar{p}_{pj}\right)^{desired}\right)^2}{\left(\psi_p\left(\bar{p}_{pj}\right)^{desired}\right)^2} \tag{17}$$

Where, $\psi_p\left(\bar{p}_{pj}\right)^{calculated}$ $and\psi_p\left(\bar{p}_{pj}\right)^{desired}$ are the mean calculated and desired operators in the process unit (sink). The desired operators are computed from the values specified in Table 6.

The application of the equations for solving the flotation circuit results in mixing of streams with unknown flows and properties and introduces bilinear terms. This case was formulated as a MINLP and solved using BARON in the General Algebraic Modeling System (GAMS) on an Intel Core i7 12th-generation processor at 2.30 GHz.

A key aspect of the methodology is the definition of the desired property values. These values should be established by considering optimal metallurgical outcomes, efficient use of flotation reagents, and feasible system parameters. For instance, as shown in Table 3, our case study indicates the presence of magnesium, calcium, copper, and sulfate ions. The target values for these ions during the process must account for the concentrations available in the water sources. An experimental design that considers the range of these properties can help determine the desired values for the flotation stages. In this context, these values were established based on the figures in Table 3 and a reasonable assumption drawn from the existing literature. The resulting values for properties used in the property integration methodology are presented in Table 6. Six properties have to be adjusted. In the case of copper ions, the cleaner 1 stage needs a lower amount of copper ions because these ions activate the residual pyrite and reduce the recovery law. The sulfate ions (SO_4^{2-}) have to be upper in cleaner 1 and ions of calcium as well. In the case of pH value, it needs to be adjusted from 8.0 to 11.5 in Cleaner1 to depress pyrite.

3. Results and analysis

This section applies the methodology to the case study. Sections 3.1 to 3.3 use the graphical procedure, which is restricted to three properties at a time. Two groups of properties are therefore examined. The first group focuses on the concentration of cations in the system, specifically magnesium (Mg^{2+}), copper (Cu^{2+}), and calcium (Ca^{2+}). The second group examines conductivity (Cond), sulfate (SO_4^{2-}), and dissolved oxygen (DO).

Sections 3.1 and 3.2 demonstrate the application of the methodology to the rougher and cleaner 1 stages, respectively, but they consider only the mixing of a single water source with the feed pulp at these stages. Section 3.3, however, illustrates the scenario of mixing two water sources with the pulp in the rougher stage.

In all of these cases, it is assumed that the total volume of each available water source is mixed with the feed pulp in each stage. In addition to this mass balance condition, the resulting mixture must remain within the feasible region (see Fig. 3a) and fall within the minimum and maximum values of AUP (see Fig. 3b).

Finally, section 3.4 presents the application of the optimization methodology, which considers a multi-objective function.

3.1. Rougher circuit

As we reviewed in the previous section, the first point of water entry occurs with the rougher pulp feed at a pulp-to-water ratio of 4, and this should be considered when interpreting subsequent results.

See Fig. 5a and Fig. 5b show the results of pulp mixing when fresh water is used in the rougher stage. The ternary diagram in Fig. 5a shows the mixture of cluster rougher inlet pulp with a cluster of fresh water; the resulting mixture lies within the feasible region, and consequently, the first condition of the methodology is fulfilled. In Fig. 5b, the AUP diagram for the rougher pulp is slightly under the maximum AUP value, in contrast to the value of fresh water AUP that is under the minimum AUP; hence, the mixing value is within the limits of AUP valid to fulfill the second condition. Note that the pulp-to-water ratio influences the final mixing value. Remember that the third condition is satisfied by the plant's mass balance. Therefore, fresh water is an alternative for the rougher circuit. Using fresh water may not be the best way to reduce

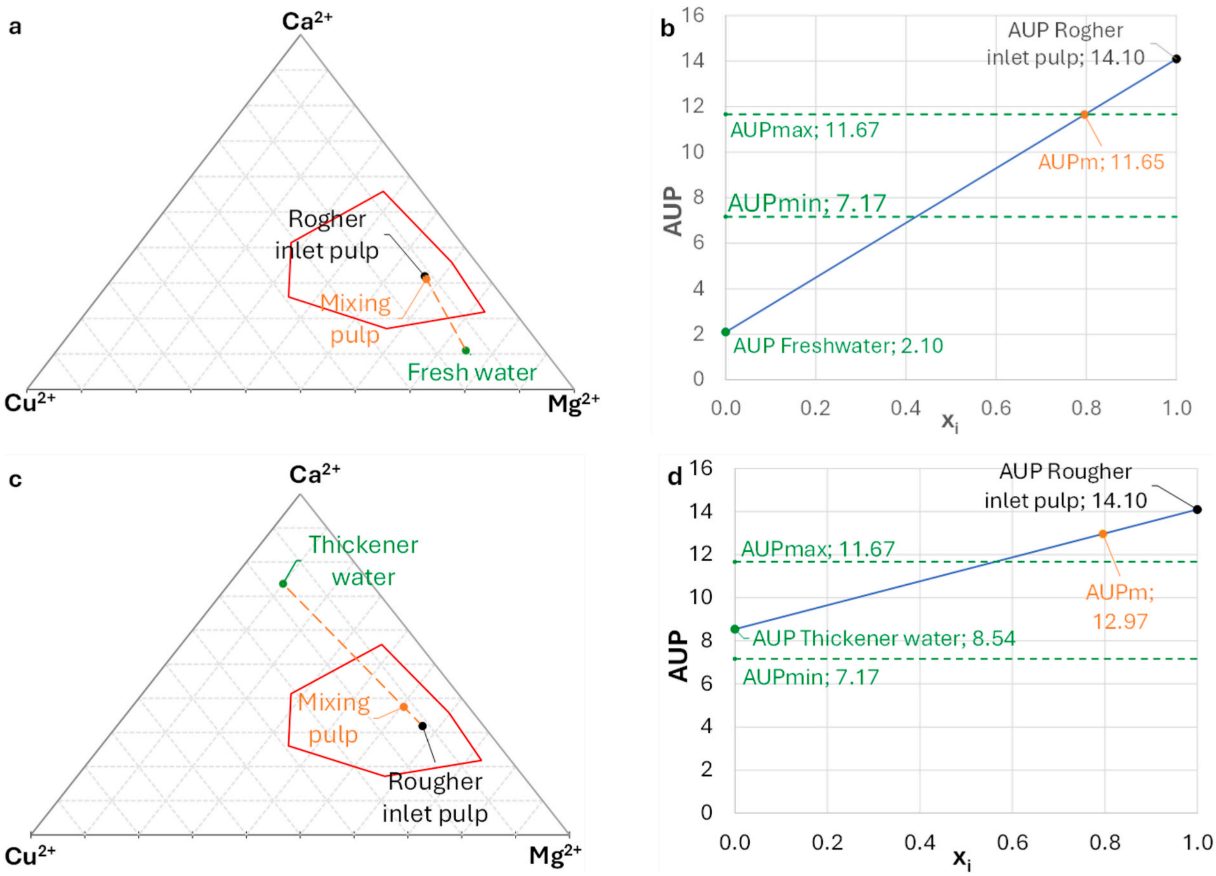

Fig. 5. Ternary diagram of Ca^{2+}, Cu^{2+} and Mg^{2+} properties showing feasible regions and location of mixing pulp stream and chart of augmented property index (AUP) required range for the rougher circuit (a) Mixing pulp using fresh water (b) Mixing stream augmented property index (AUPm) using fresh water (c) Mixing pulp using thickener water (d) Mixing stream augmented property index (AUPm) using thickener water.

consumption. Therefore, it's important to consider alternative water sources, such as thickener water or tailing pond water.

See Fig. 5c shows that the thickener water is outside the feasible region; however, the mixing pulp meets the first condition of the methodology due to the slurry/water ratio in the circuit. The AUP diagram in Fig. 5d shows that the mixing result exceeds the AUP maximum limit for the thickener water. Therefore, it does not fulfill the second condition of the methodology, and this water is not recommended for use in the rougher process.

With respect to the same circuit analyzed for Cond – SO_4^{2-}- DO properties, the mixing of rougher pulp with tailing pond water is shown in the ternary diagram of Fig. 6a. The feasible region is fulfilled for mixing all streams into the region. With respect to Fig. 6b, mixing tailing pond water with the rougher inlet pulp results in an AUP below the high limit.

Analyzing the properties Cond, SO_4^{2-}, and DO, and evaluating the properties of the process water (main source of the pulp and a mixture of all waters in different proportions), the ternary diagram in Fig. 6c shows that all mixing streams lie within the feasible region. Fig. 6d shows that the AUP value of the feed pulp is similar to that of the process water; therefore, both are outside the established region, indicating that the mixture is outside the AUP limits and that it would not be advisable to apply it directly to the process.

Based on the previous analyses, we can conclude that only the use of fresh water achieves the desired properties, although it is not the most efficient in terms of water usage. This does not imply that other types of water cannot be utilized; rather, their use hinders operation within the ideal range. As discussed later, mixing different types of water can be a more efficient approach from a water-conservation perspective.

3.2. *Cleaner 1 circuit*

As explained in the previous section, the cleaning circuit is analyzed using the property limits shown in Table 4. The particularity of the cleaning stage is that the pulp/water ratio is 5; therefore, the pulp mass relative to water predominates in the mixtures, rather than being influenced by water properties. In relation to the above, one case is analyzed for each triad of properties for the thermal oxidation water.

In this case, only the possibility of using the thermal oxidation water to generate the feed pulp in the cleaner 1 stage will be analyzed. Fig. 7 shows the results for the concentration of Mg^{2+}, Cu^{2+}, and Ca^{2+} (Fig. 7a and 7b), as well as for properties Cond, SO_4^{2-}, and DO (Fig. 7c and 7d). The combination of the cleaning pulp with the thermal oxidation water falls within the feasible region of the ternary diagram for both sets of properties, as illustrated in Fig. 7a and 7c. However, the required AUP values are not met in either case (Fig. 7b and 7d). Consequently, the use of thermal oxidation water is not appropriate for this operation.

3.3. *Rougher circuit with two water sources mixed*

In this section, we extend the analysis from section 3.1 of the rougher stage, using process water, to explore the possibility of using two water sources. As illustrated in Fig. 6c, the mixing stream falls within the feasible area of the ternary diagram; however, it does not meet the constraint regarding the maximum allowable AUP (AUPmax), since the AUP of the mixing stream exceeds this limit (Fig. 6d). To address this, we added fresh water to the initial mixing stream (pulp and process water) in order to lower the AUP of the mixture. The introduction of fresh water successfully reduces the mixing AUP to below the AUPmax limit. In Fig. 8a, the ternary diagram for the new mixing stream is shown,

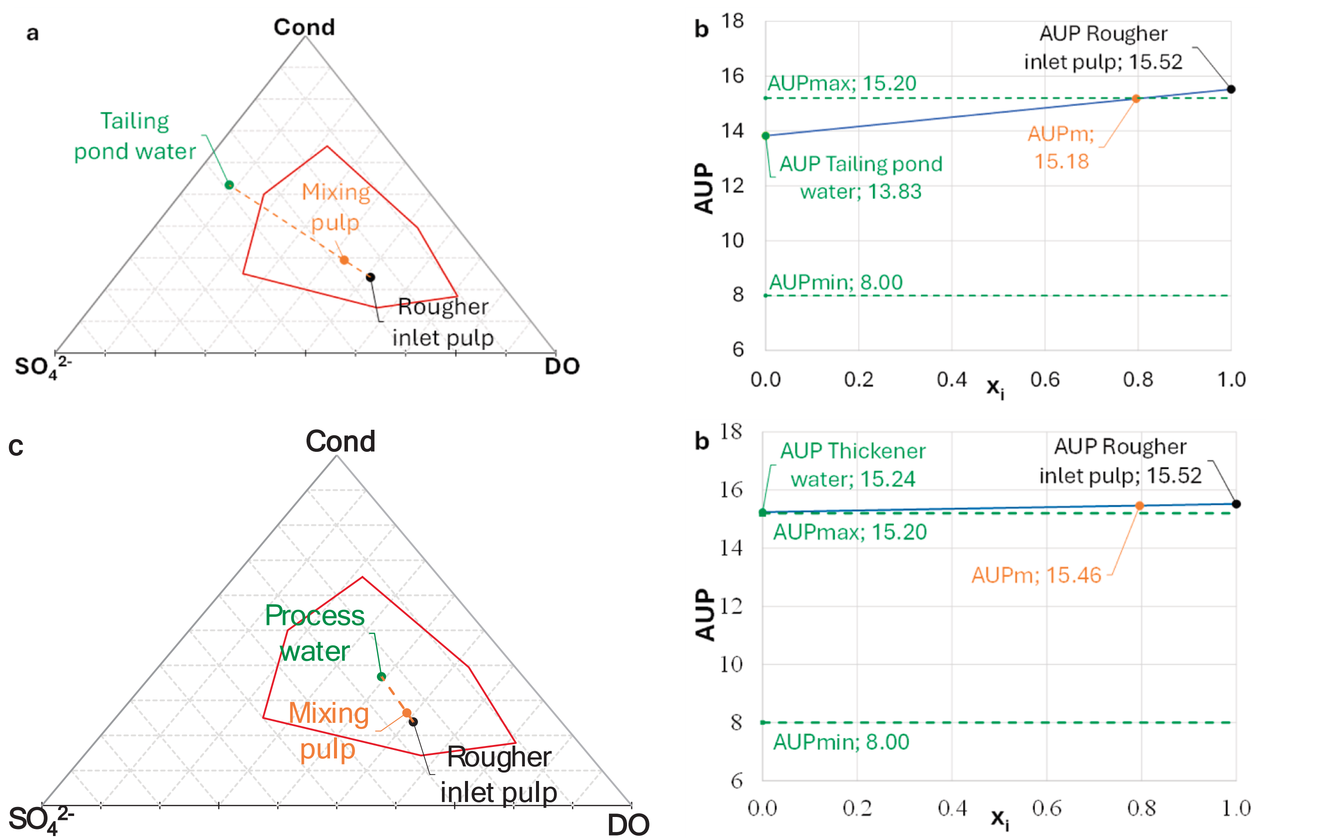

Fig. 6. Ternary diagram of Cond, SO_4^{2-} and DO properties showing feasible regions and location of mixing pulp stream and chart of augmented property index (AUP) required range for the rougher circuit (a) Mixing pulp using tailing pond water (b) Mixing stream augmented property index (AUPm) using tailing pond water (c) Mixing pulp using process water (d) Mixing stream augmented property index (AUPm) using process water.

including the process water stream, a freshwater stream, and a pulp stream. The new mixing stream remains within the feasible area, as before (Fig. 8a). However, Fig. 8b shows the AUP values for each stream relative to the AUPmax and AUPmin limits. It is clear that adding fresh water reduces the mixing AUP, resulting in an optimal water-to-pulp mixture.

Recycling process water while adding a small amount of fresh water is clearly a better option than using only fresh water, especially when considering water conservation. Using the lever rule, it can be observed that the amount of fresh water added is relatively small—just enough to achieve the desired property values in the rougher stage.

This example clearly illustrates that evaluating multiple water sources using a graphical procedure is complex and becomes unfeasible when more than three properties are considered. For this reason, an optimization-based approach is a more effective option in such situations, as will be demonstrated below.

3.4. Optimization of mass and properties results and sensitivity analysis

3.4.1. Optimization of mass and properties results

According to the mass and property optimization methodology described in section 2.4, we perform a global evaluation of the two water adding points in the flotation circuit (Fig. 2). This is, one in the rougher feeding and other in the cleaner 1 feeding, identifying the best water adding network into the circuits based on the properties of process water, thermal oxidation water, thickener water, tailing pond water. The methodology determines whether using process water or segregating available water streams is most appropriate for achieving the desired properties of the final flotation mix (Table 7), while the amount of added freshwater is held constant.

Table 7 presents the calculated property values obtained using a mixture of segregated water streams (thickener water, tailings pond water, and thermal oxidation water) or process water at the two water-addition points, the rougher and Cleaner 1 stages. For each water addition point, the deviation associated with each property operator and the corresponding total deviation are reported. As shown, the total operator deviation for the rougher stage using segregate water is lower (2.50) than using process water (23.96). However, this situation does not hold in cleaner 1, where the use of process water (0.679) is slightly lower than the use of segregate water (0.715). This happens because, for some properties, the Cleaner 1 inlet pulp itself is already close to the desired value—as with Ca^{2+}, where the pulp-dominated mixing ratio (5:1) preserves this proximity regardless of water source—while for others, such as Cu^{2+}, the process water composition is genuinely closer to the target than the segregated streams. The total operator deviation for each case of the study is 3.216 and 24.64 for the segregate water and process water, respectively, showing the benefit of using the segregate water. These results show the potential benefit of maintaining water source segregation and selectively blending the available water streams, rather than combining them into a single process water stream.

Table 7 also reports the amounts of each segregated water stream allocated to the rougher and cleaner 1 water addition points. The optimized distribution indicates that thickener water has the most favorable quality for the flotation process; therefore, it is used in a larger proportion, while freshwater consumption is maintained constant. In some industrial applications, freshwater is used not only to compensate for water losses but also to improve the physicochemical conditions affecting flotation recovery. Therefore, an additional analysis was conducted to evaluate property variations while minimizing freshwater consumption. The results of this analysis for freshwater are presented in Appendix B, which illustrates that the proposed methodology can help identify the best topological water system and analyze the trade-offs of

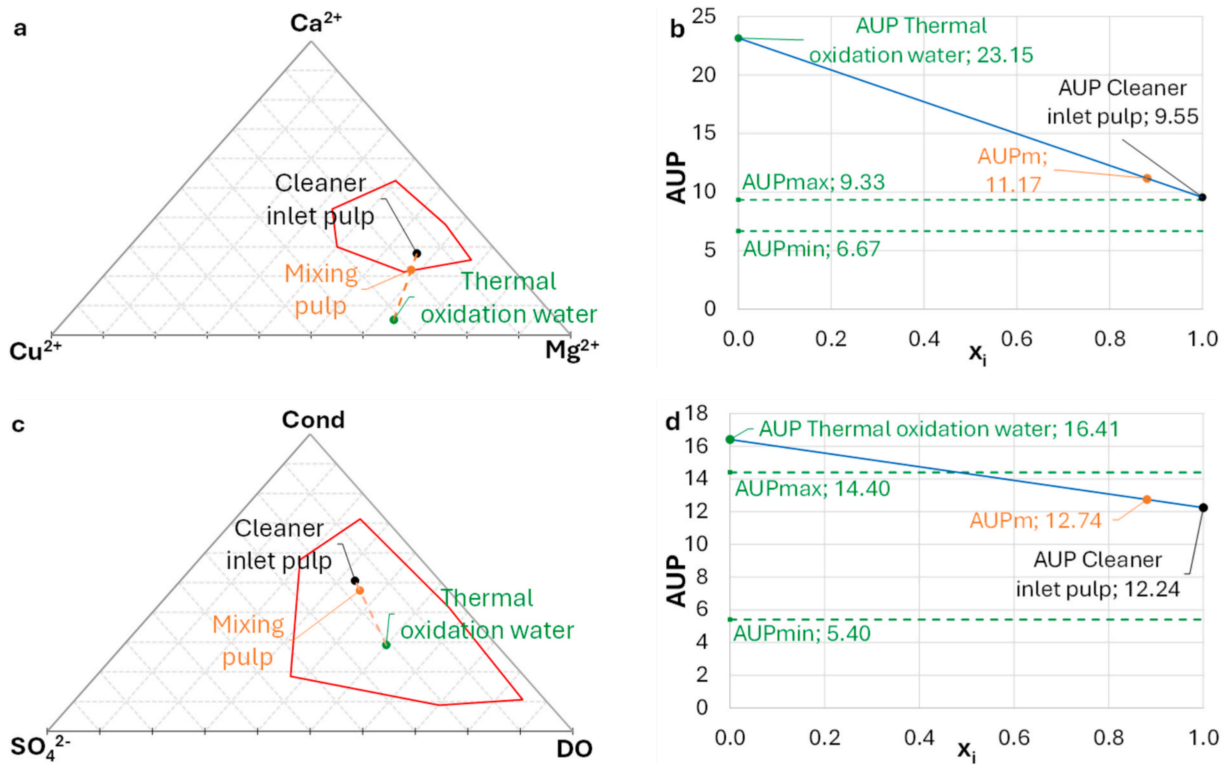

Fig. 7. Feasible regions and location of mixing pulp stream for the cleaner 1 using thermal oxidation water (a) Ternary diagram of Mg^{2+}, Cu^{2+}, and Ca^{2+} properties (b) Mixing stream augmented property index (AUPm) for Mg^{2+}, Cu^{2+}, and Ca^{2+} (c) Ternary diagram of Cond, SO_4^{2-} and DO properties (d) Mixing stream augmented property index (AUPm) for Cond, SO_4^{2-} and DO.

using freshwater.

The water allocation corresponding to the segregated water and the process-water case reported in Table 7 is graphically represented in Fig. 9a,b. This figure illustrates the distribution of water sources between the two water-addition points, namely the rougher and cleaner 1 stages. In this case, the freshwater flow rate remains constant, and it is used exclusively to compensate for water losses within the plant.

3.4.2. Sensitivity analysis on rougher and cleaner 1

The sensitivity analysis varied the concentrations of SO_4^{2-}, Mg^{2+}, and dissolved oxygen to evaluate the influence of these three properties on the total operator deviation at the rougher and cleaner 1 stages. Fig. 10a, b show the variation in SO_4^{2-} concentration from 600 to 1400 mg/L for the rougher stage and from 1300 to 1700 mg/L for the Cleaner 1 stage. In both stages, the total operator deviation exhibited a similar trend, with the segregated water strategy consistently producing lower deviation values than using process water. A comparable response was observed for Mg^{2+} concentrations ranging from 5.8 to 8.2 mg/L in the rougher stage and from 4.8 to 7.2 mg/L in the Cleaner 1 stage. For dissolved oxygen concentrations, the ranges were 7.0–9.0 mg/L in the rougher stage and 2.0–4.0 mg/L in the Cleaner 1 stage. Although different trends were observed at the two water-addition points, the curves for the segregated-water strategy remained below those obtained with process water. These results indicate that using segregated water streams is the most suitable approach for minimizing deviations from the target properties.

3.4.3. Analysis with saltwater (brackish water)

The methodology can also be applied to replace or mix continental freshwater with an alternative water source, such as brackish water (mixture of freshwater and saltwater). This replacement strategy does not aim to minimize makeup water consumption; rather, it evaluates the feasibility of using or adding a different water source based on its physicochemical properties and the extent to which its use is favorable. In this case, the replacement of saltwater with freshwater is analyzed. The properties of saltwater are described in Table 8.

See Fig. 11 illustrates the Pareto trade-off between replacing freshwater with saltwater and maintaining the target physicochemical conditions of the flotation circuit. Because the total water flow is fixed at approximately 517 t/h, decreasing freshwater necessarily increases saltwater addition. In both scenarios, greater saltwater substitution increases the total operator deviation, reflecting the growing departure from the desired pulp properties. However, the segregated water strategy consistently outperforms a single process water stream: at a given freshwater level, it achieves 20–21 fewer deviation units. For example, at a total operator deviation of about 24, the optimized segregated configuration uses approximately 327 t/h freshwater and 190 t/h saltwater. Under these conditions, a 37 % freshwater saving can be achieved using segregated water, while the water properties remain the same as with process water. Complete freshwater replacement is theoretically attainable, but only at substantially larger deviations, around 140 and 160 for segregated and process water, respectively. Thus, W-PIM/CP provides a quantitative basis for comparing alternative water sources and identifying blends that balance water substitution with control of metallurgical properties.

3.5. Considerations for industrial implementation

Regarding the practical implementation of the W-PIM/CP framework, note that the current model is primarily intended for strategic network synthesis and design. Future iterations of this work will expand the scope to include dynamic mass and property balances, as well as inventory management within the water storage infrastructure. In an industrial setting, large-scale process water ponds and thickeners function as significant hydraulic and chemical buffers that naturally dampen high-frequency fluctuations in water quality parameters. This inherent

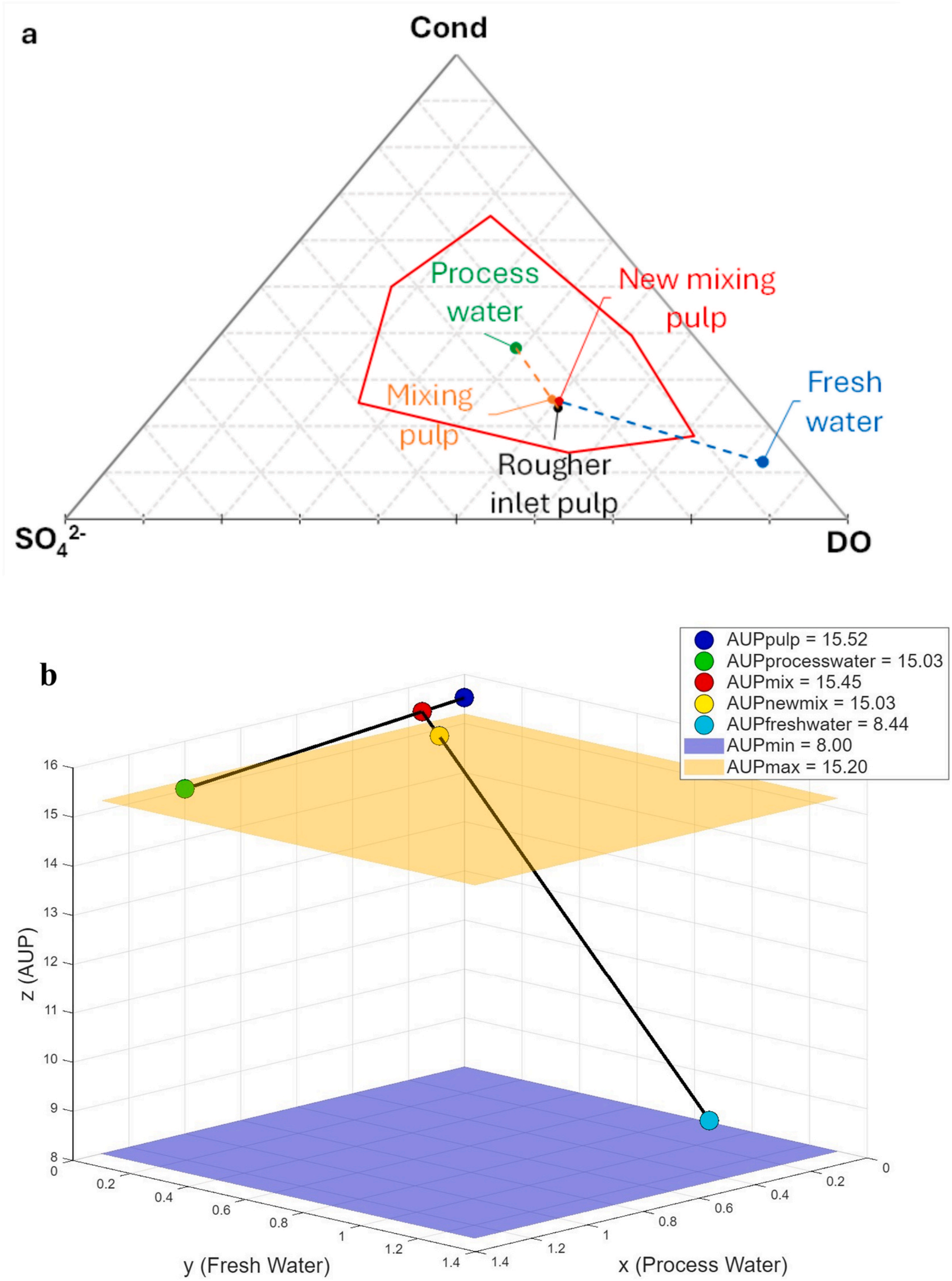

Fig. 8. (a) Ternary diagram of Cond, SO_4^{2-}, and DO showing feasible region and location of mixing pulp stream for the rougher circuit using process and fresh water. (b) Location of mixing stream augmented property index (AUPm) value using process and fresh water in a three-dimensional graphic chart of the required range.

dampening effect prevents abrupt deviations in the chemical environment of the flotation circuit, allowing for the framework's application through periodic offline laboratory analyses or semi-continuous monitoring. Even considering the limitations of current sensor technologies, the proposed methodology represents a substantial advancement over the prevailing industrial status quo, in which diverse water streams are typically commingled with minimal or nonexistent tracking of their functional properties.

The feasible regions used in this case study were defined from literature-derived property ranges associated with favorable chalcopyrite flotation and pyrite depression, together with the measured chemical domain of the available pulp and water streams. Therefore, these limits should be interpreted as illustrative bounds for analyzing the W-PIM/CP methodology, rather than as fixed thresholds applicable to all flotation plants. From a practical perspective, the feasible property windows required for industrial implementation must be calibrated for each operation, since the metallurgical response to water quality depends on ore mineralogy, mineral dissolution, galvanic interactions, reagent scheme, recycled-water composition, pH control strategy, and plant operating conditions. Consequently, site-calibrated bounds should

Table 7
Property and operator deviation values for rougher and cleaner 1 inlets and water distribution in the analyzed circuit.

Property	Units	Rougher Desired value	Segregate water Calculated value	Segregate water Operator deviation	Process water Calculated value	Process water Operator deviation	Cleaner 1 Desired value	Segregate water Calculated value	Segregate water Operator deviation	Process water Calculated value	Process water Operator deviation
Conductivity	µS/cm	*4000.00*	3795.02	0.0026	4077.00	0.0004	*4000.00*	5994.74	0.2487	5534.11	0.1471
Dissolved Oxygen	mg/L	*8.00*	7.51	0.0038	7.51	0.0038	*3.00*	4.74	0.3352	4.85	0.3807
Mg^{2+}	mg/L	*7.00*	10.29	0.2208	10.04	0.1887	*6.00*	7.28	0.0454	7.47	0.0597
Ca^{2+}	mg/L	*200.00*	441.22	1.4547	487.14	2.0613	*300.00*	360.74	0.0410	293.97	0.0004
Cu^{2+}	mg/L	*0.25*	0.157	0.1384	0.160	0.1296	*0.15*	0.162	0.0064	0.154	0.0007
SO_4^{2-}	mg/L	*1000.00*	1825.62	0.6817	1918.82	0.8442	*1500.00*	1218.69	0.0352	1056.82	0.0873
pH		*8.00*	8.00	0.000	8.75	20.73	*11.50*	11.52	0.0026	11.52	0.0026
Sum of operator deviations				2.50		23.96			0.715		0.679
Water Consumption											
Freshwater	tph		517.09		0.00			0.00		517.09	
Thermal oxidation water	tph		130.00		0.00			0.00		0.00	
Thickener water	tph		575.92		0.00			821.08		0.00	
Tailing pond water	tph		300.80		0.00			174.20		0.00	
Process water	tph		0.00		1523.81			0.00		478.19	
Sum of used water			1523.81		1523.81			995.28		995.28	

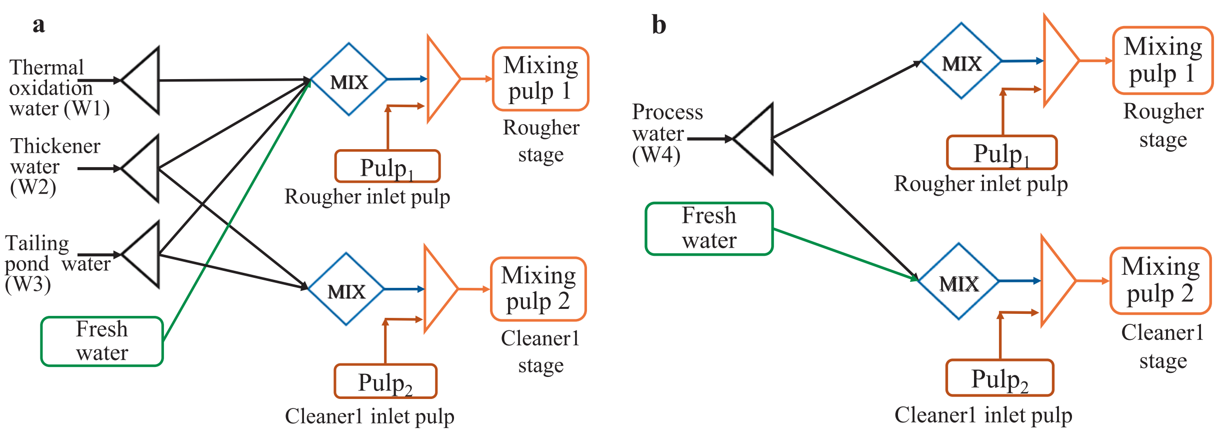

Fig. 9. Optimal water network configuration derived from the MINLP model, illustrating mixing and recycling strategies under the W-PIM/CP framework.

be obtained through bench flotation tests, plant surveys, historical metallurgical data, or a design of experiments linking water properties with recovery, grade, selectivity, and reagent consumption. On the other hand, the successful industrial deployment of W-PIM/CP relies on a synergistic approach between metallurgy and systems engineering. The metallurgical response to water quality cannot be generalized across all concentration plants, because it depends on ore mineralogy, valuable and gangue mineral associations, reagent scheme, pulp chemistry, and the residence time of recycled waters. A preliminary experimental phase using DoE is essential to calibrate the optimal property windows. Once these metallurgical targets are established, they can be used as the optimization tool to allocate and blend the available water sources while maintaining the process as close as possible to the desired physico-chemical domain.

It should be noted that the mathematical clustering of properties typically assumes a linear superposition via property operators. However, in complex mineral pulps, interactions between ions and residual reagents often exhibit non-linear behaviors, such as ion speciation, synergistic precipitation, or antagonistic effects on collector adsorption. Reagent-related effects represent a relevant boundary of the current W-PIM/CP formulation. The present model considers inorganic ions and physicochemical properties such as pH, dissolved oxygen, conductivity, and selected dissolved species; however, collectors, frothers, depressants, pH modifiers, flocculants, and their degradation products may also affect mineral hydrophobicity, bubble-particle attachment, froth stability, redox conditions, and reagent adsorption. These effects may be partially captured through measured pulp properties, but they are not explicitly included as independent property operators in this proof-of-concept model. Consequently, the definition of the 'Feasible Region' in the W-PIM/CP framework must be grounded in experimental data or rigorous thermodynamic simulations that reflect the specific solution matrix and key variables, such as pH and ionic strength. By establishing these metallurgical windows based on the actual chemical environment of the pulp, the framework can effectively guide the mixing of recycled streams. This functionality-based approach, despite the challenges posed by non-linear chemical interactions, represents a substantial improvement over traditional mass-balance management, which fails to account for water-quality deviations and their impact on mineral-separation kinetics. Furthermore, this systematic approach enables the identification of the precise threshold at which freshwater

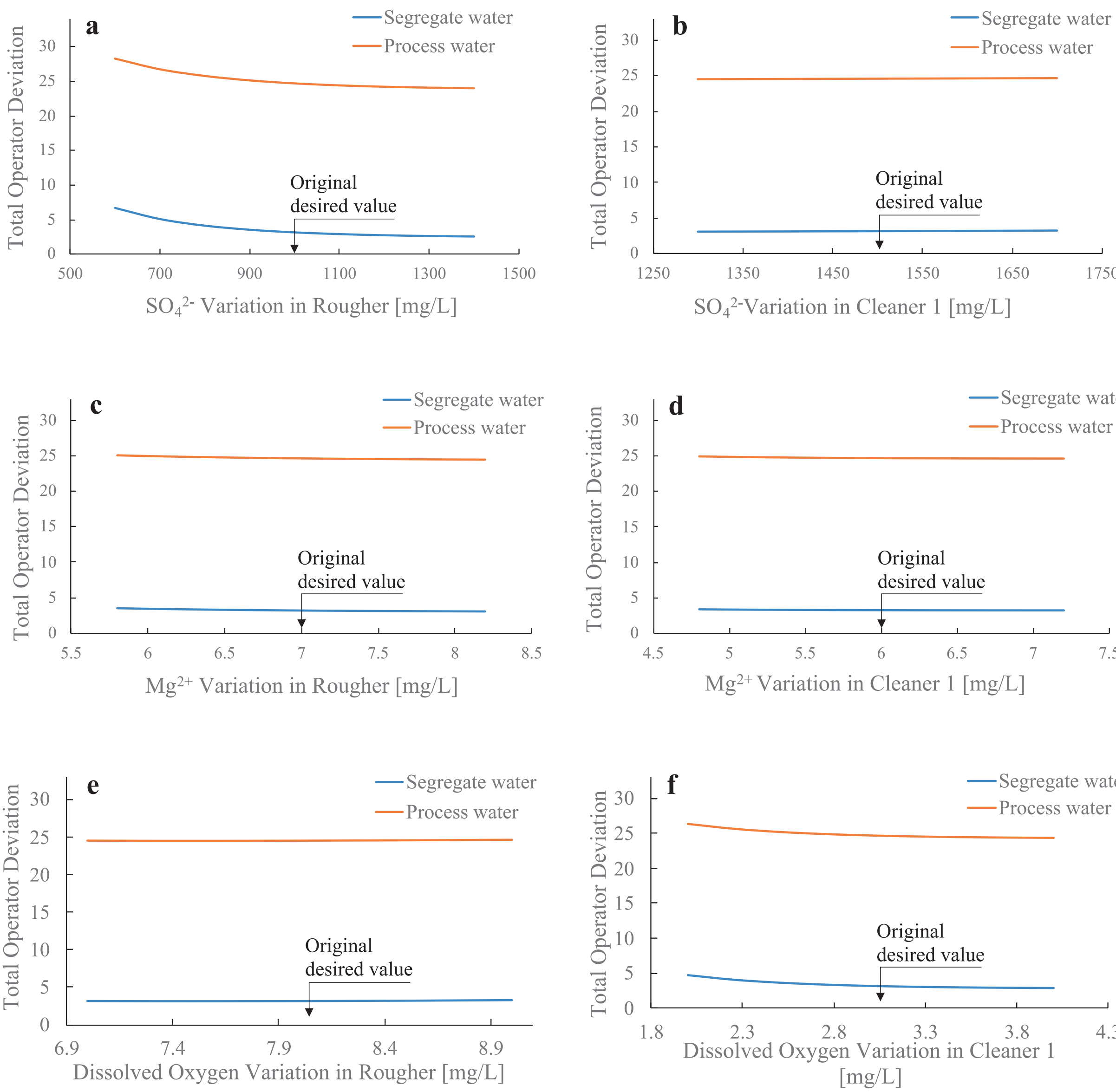

Fig. 10. Sensitivity analysis of rougher and cleaner 1 stage for process water and segregate water (thickener, tailings pond, and thermal oxidation water). (a,b) Impact of target $SO_4{}^{2-}$ on total operator deviation, (c,d) Impact of target Mg^{2+} on total operator deviation, (e,f) Impact of target and Dissolved Oxygen on total operator deviation.

Table 8
Properties for saltwater (typical values for seawater).

	SO_4^{2-} (mg/L)	DO (mg/L)	Cu^{2+} (mg/L)	Mg^{2+} (mg/L)	Ca^{2+} (mg/L)	Conductivity (μS/cm)	pH
Saltwater	2750	7.40	0.001	1300	420	53,000	8.1

reduction begins to jeopardize metallurgical stability, a critical decision-making capability that goes beyond simple volumetric balances.

Implementing the W-PIM/CP framework requires evaluating CAPEX against long-term operational value. Traditional water networks often rely on large, centralized process water ponds, while this framework choice favors segregated storage. Although multiple storage units and valve systems may increase initial construction costs, these can be partially offset by more efficient plant layouts that reduce piping distances and pumping energy. Crucially, feasibility rests on two benefits: a significant reduction in OPEX through the optimized use of reagents, such as pH modifiers and collectors, which are often overdosed to counteract water impurities, and a substantial increase in revenue due to enhanced metallurgical stability. By precisely controlling the chemical environment of the pulp, the plant can avoid recovery losses and grade fluctuations associated with unmanaged recycled water. This shifts water management from a cost center to a strategic tool for maximizing the overall net present value (NPV) of the concentration process.

A key advantage of the framework is its ability to reduce the dynamic complexity of the flotation circuit. Currently, most operations combine all recycled water sources into a centralized pond, creating a chemical environment where unpredictable interactions, such as reactions between fluctuating pH levels in tailings water and residual reagents in thickener overflows, often occur. We argue that much of the perceived instability in recycled water quality is a direct result of this indiscriminate mixing. By implementing a segregated storage strategy based on property clusters, the plant can isolate streams with compatible attributes, thereby reducing chemical noise and overall system uncertainty. Although this functionality-based approach simplified the model of the complex water-metal nexus, it provides a superior decision-making structure compared to traditional methods, enabling more robust

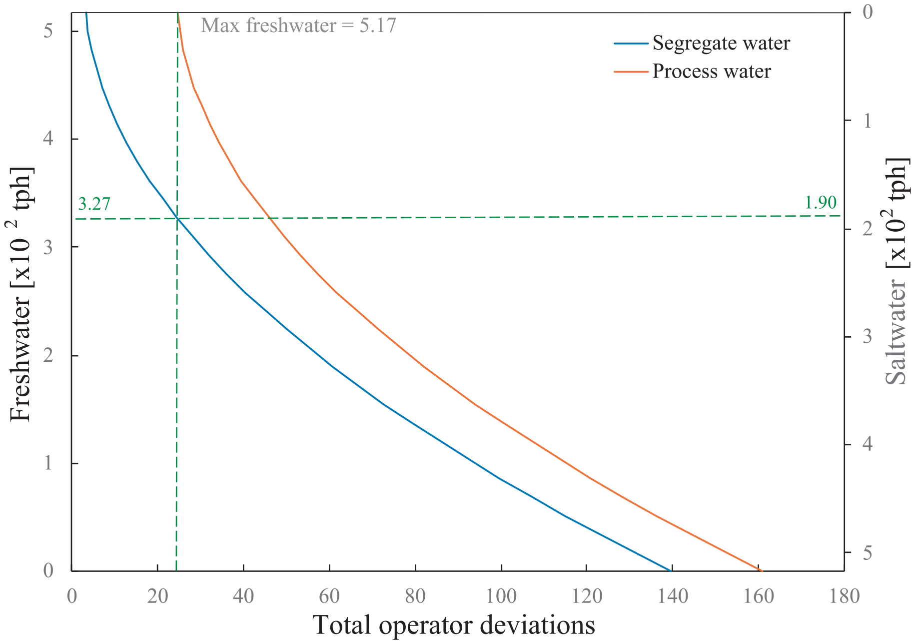

Fig. 11. Pareto curve for the optimization approach, focusing on adding salt water to replace the use of freshwater while satisfying the desired properties.

control over the flotation chemical environment.

3.6. Economic sensitivity analysis

A conceptual CAPEX assessment was performed to quantify the incremental cost of implementing the W-PIM/CP segregation logic by using two functionally separate process-water pools rather than a single centralized pond. Both configurations were sized for the same total storage capacity, with the segregated alternative distributing 1524 m^3/h to the rougher pool and 995 m^3/h to the cleaner pool. Pool volumes were sized to provide 48 h of operating inventory, resulting in a total storage capacity of 120,916 m^3 across both configurations. Pool costs were estimated using the six-tenths scaling rule, and pump station costs were calculated from the hydraulic power equation and scaled by installed power. The resulting incremental CAPEX was estimated at 1.91 MUSD (Class 5 conceptual estimate, ±50 %, range 0.96–2.87 MUSD). Civil works and lining for the pools accounted for 82 % of the increase; pump stations accounted for the remaining 18 %.

Because the framework is presented as a proof of concept, the economic assessment is framed as a sensitivity analysis: it estimates the recovery improvement required to offset the incremental CAPEX, rather than predicting a specific NPV. Two complementary metrics are reported. Using a discounted cash flow criterion over a five-year horizon at an 8 % discount rate, the threshold improvement in copper recovery that makes the NPV of the incremental investment equal to zero is 0.019 percentage points. As a complementary view, Table 9 reports the simple payback period (undiscounted) for three illustrative recovery-improvement scenarios; even in the most conservative scenario of 0.5 percentage points, the payback period is on the order of two months. The threshold recovery improvement required to offset the incremental CAPEX is therefore small relative to the recovery sensitivities to water quality reported in the flotation literature. All equations, assumptions, and calculations are detailed in Appendix A.

4. Conclusions and future work

4.1. Conclusions

This work proposes the Water Property Integration Method for Concentration Plants (W-PIM/CP), a framework that complements conventional volumetric water balances by tracking physical and chemical water-quality properties (pH, dissolved oxygen, conductivity, and key ionic species) across the water network of a mineral concentration plant. The framework was illustrated on a sulfide flotation circuit as a proof of concept.

The main results of the case study are the following:

- Ternary cluster diagrams are a useful graphical aid when up to three properties are tracked, but become limited at higher dimensionality. The MINLP formulation is required to allocate water sources in multi-property settings, where bilinear terms arise from the simultaneous optimization of flows and property values.
- Applied to the rougher and cleaner 1 stages, the model shows that recycled water sources (thickener, tailings pond, and thermal oxidation water) can be assigned to specific flotation stages provided that their combined properties fall within the feasibility region defined by the target property windows. The cleaner 1 stage, in particular, can be operated primarily on recycled water, subject to control of insoluble solids.
- Centralized commingling of all recycled streams into a single pool produced the largest deviations from the target property values at each flotation stage and was the least favorable configuration among those tested. Allocating water sources into functional pools through the W-PIM/CP model offers a more controlled alternative.

Table 9
Simple (undiscounted) payback period for Δ CAPEX as a function of recovery improvement.

Scenario	Recovery improvement ΔR (pp)	Annual revenue gain (MUSD/yr)	Payback time for ΔCAPEX (yr)	Payback period on ΔCAPEX (weeks)
Low scenario	0.50	12.38	0.15	8.0
Medium scenario	1.00	24.76	0.08	4.0
High Scenario	1.50	37.14	0.05	2.7

- The Pareto curve shows that using segregated water streams provides greater flexibility for incorporating alternative water sources while preserving physicochemical conditions closer to the desired metallurgical operating range than using a single commingled process water stream.
- A conceptual CAPEX assessment (Class 5, ±50 %) of the segregated configuration relative to a centralized one indicates an incremental cost of 1.91 MUSD. Under a discounted-cash-flow criterion (5-year horizon, 8 % discount rate), the threshold improvement in copper recovery that offsets this incremental cost is 0.019 percentage points; feasibility therefore depends primarily on metallurgical validation rather than on capital cost.

The framework is presented as a proof of concept under literature-derived property windows. Industrial deployment would require site-specific calibration of those windows through bench-scale flotation tests, plant surveys, historical data, or design of experiments, as discussed in Section 3.5.

4.2. Future studies

Several extensions of the W-PIM/CP framework deserve further investigation:

- *Site-specific calibration of property windows.* The feasibility regions used in this work were derived from ranges reported in the literature. A systematic procedure for defining target property values from a combination of bench flotation tests, design of experiments, and historical plant data is required before the framework can be deployed at an industrial scale. Such a procedure should account for ore mineralogy, mineral dissolution chemistry, and the reagent scheme of the operation.
- *Coupling with reagent consumption.* Adverse water properties (high ionic strength, low dissolved oxygen, pH drift) are typically compensated for by adjusting the dosages of collector, depressant, or pH modifier. Quantifying these compensations as functions of water-quality variables and including them in the MINLP objective would extend the framework to jointly optimize water allocation and reagent OPEX.
- *Dynamic operation on a fixed network topology.* The present formulation is a steady-state synthesis model. Industrial circuits experience time-varying ore mineralogy and recycled-water composition, so a dynamic version of the framework, operating on a fixed network topology, could serve as a regulatory layer to adjust flow rates and maintain pulp properties within target windows in response to upstream disturbances.
- *Non-conservative property operators.* Some water-quality variables, particularly those associated with residual organic reagents and Total Organic Carbon (TOC), are not conservative during mixing due to degradation and reaction. A given TOC value in the thickener overflow may correspond to a different mixture of intermediate species than the same TOC value in the tailings pond. Extending the property operators to capture these transformations is a natural next step toward dynamic property prediction.
- *Microbial activity as a water-quality property.* Microbial communities present in flotation plants can affect mineral surfaces and have been studied as potential bioreagents (Kinnunen et al., 2020; Arias et al., 2023). Incorporating microbial activity as an additional property within the W-PIM/CP framework would require both characterization protocols and a suitable property operator.
- *Integration with dewatering operations.* Thickeners and filters are commonly modeled as passive solid–liquid separation units, but their flocculant chemistry and operating conditions modify the water that re-enters the flotation circuit. Treating these units as active property-modifying stages would close the loop between flotation and water recovery (Unesi et al., 2014).

CRediT authorship contribution statement

Luis A. Cisternas: Writing – review & editing, Supervision, Project administration, Methodology, Funding acquisition, Data curation, Conceptualization. **Israel Ponce-Lizarazu:** Writing – original draft, Methodology, Investigation. **Marinka Silva:** Writing – original draft, Investigation, Data curation, Conceptualization. **Nathalie Jamett:** Methodology, Investigation, Conceptualization. **Andrzej Kraslawski:** Writing – review & editing, Validation, Supervision.

Declaration of competing interest

The authors declare that they have no known competing financial interests or personal relationships that could have appeared to influence the work reported in this paper.

Acknowledgments

We also acknowledge the financial support of ANID (National Agency for Research and Development, Chile) through grant CIA250010 and the Regional Government of Antofagasta (Chile) through the project “Fortalecimiento del Ecosistema de CTCI a través del Doctorado en Ingeniería de Procesos de Minerales” (COD BIP 40067594-0). Additionally, I. Ponce acknowledges the research infrastructure and institutional support provided by the Doctoral Program in Mineral Process Engineering at the University of Antofagasta, Chile.

Appendix A. Supplementary data

Supplementary data to this article can be found online at https://doi.org/10.1016/j.mineng.2026.110835.

Data availability

No data was used for the research described in the article.

References

Aaltonen, A., Izart, C., Lyyra, M., Lang, A., Saari, E., Dahl, O., 2023. Simulating the Impact of Ore and Water Quality on Flotation Recovery during the Life of a Mine. Minerals 13, 1230. https://doi.org/10.3390/min13091230.

Arias, D., Salazar-Ardiles, C., Andrade, D.C., Rivas, M., Panico, A., Race, M., Cisternas, L. A., Dorador, C., 2023. The microbial world in copper sulfide flotation plants (CSFP): Novel insights into bacterial communities and their application as potential pyrite bioreagents. Environ. Res. 218, 114904. https://doi.org/10.1016/j.envres.2022.114904.

Bicak, O., Cakir, E., Ozcelik, S., Ekmekci, Z., 2023. The Impact of Pulp Temperature on the Flotation Performance of Copper-Lead-Zinc Sulphide Ore. Minerals 13, 1181. https://doi.org/10.3390/min13091181.

Castellón, C.I., Toro, N., Gálvez, E., Robles, P., Leiva, W.H., Jeldres, R.I., 2022. Froth Flotation of Chalcopyrite/Pyrite Ore: a critical Review. Materials 15, 6536. https://doi.org/10.3390/ma15196536.

Chen, C., Lee, J., Ng, D.K.S., Foo, D.C.Y., 2010. A unified model of property integration for batch and continuous processes. AIChE J 56, 1845–1858. https://doi.org/10.1002/aic.12116.

Chi, X., Guo, Y., Zhong, S., Li, G., Lv, X., 2020. Molecular modelling and synthesis of a new collector *O* -butyl *S* -(1-chloroethyl)carbonodithioate for copper sulfide ore and its flotation behavior. RSC Adv. 10, 3520–3528. https://doi.org/10.1039/C9RA09648E.

Cisternas, L.A., Gálvez, E.D., 2018. The use of seawater in mining. Miner. Process. Extr. Metall. Rev. 39, 18–33. https://doi.org/10.1080/08827508.2017.1389729.

Cochilco, 2023. Consumo de Agua en la Minería del Cobre. Gobierno de Chile, Santiago, Chile.

Corin, K.C., Charamba, A., Manono, M.S., 2024. Water quality impact on flotation Response: a focus on specific ions and temperature. Miner. Eng. 207, 108549. https://doi.org/10.1016/j.mineng.2023.108549.

Cruz, C., Botero, Yesica.L., Jeldres, R.I., Uribe, L., Cisternas, L.A., 2022. Current Status of the Effect of Seawater Ions on Copper Flotation: Difficulties, Opportunities, and Industrial Experience. Miner. Process. Extr. Metall. Rev. 43, 545–563. Doi: 10.1080/08827508.2021.1900175.

De Lima, J.P.M., Amaral, M.C.S., De Lima, S.C.R.B., 2025. Sustainable water management in the mining industry: Paving the way for the future. J. Water Process Eng. 71, 107239. https://doi.org/10.1016/j.jwpe.2025.107239.

Deng, C., Shi, C., Feng, X., Foo, D.C.Y., 2016. Flow Rate Targeting for Concentration- and Property-based Total Water Network with Multiple Partitioning Interception units. Ind. Eng. Chem. Res. 55, 1965–1979. https://doi.org/10.1021/acs.iecr.5b03203.

Ding, H., Feng, X., Wu, Y., Zhang, Z., 2020. Water Network Integration of a Printing and Dyeing Plant. Process Integr. Optim. Sustain. 4, 121–133. https://doi.org/10.1007/s41660-019-00098-3.

Dzingai, M., Manono, M., Corin, K., 2020. Simulating the effect of Water Recirculation on Flotation through Ion-Spiking: effect of Ca2+ and Mg2+. Minerals 10, 1033. https://doi.org/10.3390/min10111033.

El-Bacha, R., Salhi, A., Abderrafia, H., Rabi, S., 2025. Optimising water use in copper flotation with the design of experiments and machine learning. South Afr. J. Sci. 121. https://doi.org/10.17159/sajs.2025/16239.

El-Halwagi, M.M., 2017. Property Integration, in: Sustainable Design Through Process Integration. Elsevier, pp. 283–306. Doi: 10.1016/B978-0-12-809823-3.00010-2.

El-Halwagi, M.M., Glasgow, I.M., Qin, X., Eden, M.R., 2004. Property integration: Componentless design techniques and visualization tools. AIChE J 50, 1854–1869. https://doi.org/10.1002/aic.10305.

Fan, P., Tong, X., Xie, X., Song, Q., Ma, Y., Han, B., Fu, H., Lu, Z., 2025. Selective Oxidation Depression of Copper-Activated Sphalerite by H2O2 during Chalcopyrite Flotation. Metals 15, 813. https://doi.org/10.3390/met15070813.

Feng, Q., Yang, W., Chang, M., Wen, S., Liu, D., Han, G., 2024. Advances in depressants for flotation separation of Cu-Fe sulfide minerals at low alkalinity: a critical review. Int. J. Miner. Metall. Mater. 31, 1–17. https://doi.org/10.1007/s12613-023-2709-3.

Foroutan, A., Abbas Zadeh Haji Abadi, M., Kianinia, Y., Ghadiri, M., 2021. Critical importance of pH and collector type on the flotation of sphalerite and galena from a low-grade lead–zinc ore. Sci. Rep. 11, 3103. Doi: 10.1038/s41598-021-82759-3.

Gálvez, E.D., Cruz, R., Robles, P.A., Cisternas, L.A., 2014. Optimization of dewatering systems for mineral processing. Miner. Eng. 63, 110–117. https://doi.org/10.1016/j.mineng.2014.01.026.

Gao, Z., Jiang, Z., Sun, W., Gao, Y., 2021. Typical roles of metal ions in mineral flotation: a review. Trans. Nonferrous Met. Soc. China 31, 2081–2101. https://doi.org/10.1016/S1003-6326(21)65640-6.

Göktepe, F., 2002. Effect of pH on pulp potential and sulphide mineral flotation. Turk. J Eng Env. Sci 26, 309–318.

Grano, S.R., Lauder, D.W., Johnson, N.W., Ralston, J., 1997. An investigation of Galena recovery problems in the Hilton concentrator of Mount Isa Mines Limited. Australia. Miner. Eng. 10, 1139–1163. https://doi.org/10.1016/S0892-6875(97)00100-3.

Hirajima, T., Suyantara, G.P.W., Ichikawa, O., Elmahdy, A.M., Miki, H., Sasaki, K., 2016. Effect of Mg2+ and Ca2+ as divalent seawater cations on the floatability of molybdenite and chalcopyrite. Miner. Eng. 96–97, 83–93. https://doi.org/10.1016/j.mineng.2016.06.023.

Jeldres, R.I., Forbes, L., Cisternas, L.A., 2016. Effect of Seawater on Sulfide Ore Flotation: a Review. Miner. Process. Extr. Metall. Rev. 37, 369–384. https://doi.org/10.1080/08827508.2016.1218871.

Jiménez-Gutiérrez, A., Sandate-Trejo, M., El-Halwagi, M., 2014. An MINLP Model that includes the effect of Temperature and Composition on Property Balances for Mass Integration Networks. Processes 2, 675–693. https://doi.org/10.3390/pr2030675.

Kazantzi, V., 2006. Novel visualization and algebraic techniques for sustainable development through property integration (Ph.D. Dissertation). Texas A&M University.

Kinnunen, P., Miettinen, H., Bomberg, M., 2020. Review of potential Microbial Effects on Flotation. Minerals 10, 533. https://doi.org/10.3390/min10060533.

Kuopanportti, H., Suorsa, T., Pöllänen, E., 1997. Effects of oxygen on kinetics of conditioning in sulphide ore flotation. Miner. Eng. 10, 1193–1205. Doi: 10.1016/S0892-6875(97)00106-4.

Leiva González, J., Onederra, I., 2022. Environmental Management strategies in the Copper Mining Industry in Chile to Address Water and Energy Challenges—Review. Mining 2, 197–232. https://doi.org/10.3390/mining2020012.

Levay, G., Smart, R.S.C., Skinner, W.M., 2001. The impact of water quality on flotation performance. J. S. Afr. Inst. Min. Metall. 101, 69–75.

Li, A.-H., Zhang, L., Liu, Z.-Y., 2022. Synthesis of property-based total water systems with multiple interceptors by using operator potential concepts. Chem. Eng. Res. Des. 184, 338–348. https://doi.org/10.1016/j.cherd.2022.06.016.

Lin, Z., Wang, P., Tang, L., Wang, Z., Mckechnie, J., Li, B., Chen, W.-Q., Chan, F.K.S., 2025. Public water risk concerns triggered by energy-transition-mineral mining. Resour. Environ. Sustain. 19, 100196. https://doi.org/10.1016/j.resenv.2025.100196.

Liu, Q., Zhang, Y., 2000. Effect of calcium ions and citric acid on the flotation separation of chalcopyrite from galena using dextrin. Miner. Eng. 13, 1405–1416. https://doi.org/10.1016/S0892-6875(00)00122-9.

Liu, W., Moran, C.J., Vink, S., 2013. A review of the effect of water quality on flotation. Miner. Eng. 53, 91–100. https://doi.org/10.1016/j.mineng.2013.07.011.

Lucay, F., Cisternas, L.A., Gálvez, E.D., 2015. Global sensitivity analysis for identifying critical process design decisions. Chem. Eng. Res. Des. 103, 74–83. https://doi.org/10.1016/j.cherd.2015.06.015.

Manono, M.S., Corin, K.C., Wiese, J.G., 2012. An investigation into the effect of various ions and their ionic strength on the flotation performance of a platinum bearing ore from the Merensky reef. Miner. Eng. 36–38, 231–236. https://doi.org/10.1016/j.mineng.2012.03.035.

Mu, Y., Peng, Y., 2019. The effect of saline water on copper activation of pyrite in chalcopyrite flotation. Miner. Eng. 131, 336–341. https://doi.org/10.1016/j.mineng.2018.11.032.

Mu, Y., Peng, Y., Lauten, R.A., 2016. The depression of pyrite in selective flotation by different reagent systems – a Literature review. Miner. Eng. 96–97, 143–156. https://doi.org/10.1016/j.mineng.2016.06.018.

Nápoles-Rivera, F., Ponce-Ortega, J.M., El-Halwagi, M.M., Jiménez-Gutiérrez, A., 2010. Global optimization of mass and property integration networks with in-plant property interceptors. Chem. Eng. Sci. 65, 4363–4377. https://doi.org/10.1016/j.ces.2010.03.051.

Ng, D.K.S., Foo, D.C.Y., Rabie, A., El-Halwagi, M.M., 2008. Simultaneous synthesis of property-based water reuse/recycle and interception networks for batch processes. AIChE J 54, 2624–2632. https://doi.org/10.1002/aic.11578.

October, L.L., Corin, K.C., Manono, M.S., Schreithofer, N., Wiese, J.G., 2020. A fundamental study considering specific ion effects on the attachment of sulfide minerals to air bubbles. Miner. Eng. 151, 106313. https://doi.org/10.1016/j.mineng.2020.106313.

Owusu, C., Abreu, B.E., Skinner, S., Addai-Mensah, W., Zanin, J., 2014. The influence of pyrite content on the flotation of chalcopyrite/pyrite mixtures. Miner. Eng. 55, 87–95. https://doi.org/10.1016/j.mineng.2013.09.018.

Raghavan, S., Hsu, L.L., 1984. Factors affecting the flotation recovery of molybdenite from porphyry copper ores. Int. J. Miner. Process. 12, 145–162. https://doi.org/10.1016/0301-7516(84)90026-7.

Rios, L.A., Barraza, M.J., Robles, P.A., Quezada, G.R., 2025. Chalcopyrite Flotation, Molecular Design and Smart Industry: a Review. Int. J. Mol. Sci. 26, 3613. https://doi.org/10.3390/ijms26083613.

Ruffino, B., Campo, G., Crutchik, D., Reyes, A., Zanetti, M., 2022. Drinking Water Supply in the Region of Antofagasta (Chile): a Challenge between past, present and Future. Int. J. Environ. Res. Public Health 19, 14406. https://doi.org/10.3390/ijerph192114406.

Sandate-Trejo, M.D.C., Jiménez-Gutiérrez, A., El-Halwagi, M., 2014. Property integration models with interdependence mixing operators. Chem. Eng. Res. Des. 92, 3038–3045. https://doi.org/10.1016/j.cherd.2014.06.025.

Shelley, M.D., El-Halwagi, M.M., 2000. Component-less design of recovery and allocation systems: a functionality-based clustering approach. Comput. Chem. Eng. 24, 2081–2091. https://doi.org/10.1016/S0098-1354(00)00578-0.

Shen, W.Z., Fornasiero, D., Ralston, J., 2001. Flotation of sphalerite and pyrite in the presence of sodium sulfite. Int. J. Miner. Process. 63, 17–28. https://doi.org/10.1016/S0301-7516(00)00067-3.

Sinche-Gonzalez, M., Fornasiero, D., 2021. Understanding the effect of sulphate in mining-process water on sulphide flotation. Miner. Eng. 165, 106865. https://doi.org/10.1016/j.mineng.2021.106865.

Sinche-Gonzalez, M., Fornasiero, D., Zanin, M., 2016. Flotation of Chalcopyrite and Molybdenite in the Presence of Organics in Water. Minerals 6, 105. https://doi.org/10.3390/min6040105.

Soufiabadi, A.M., Dehghan, R., Nejadaria, M., Safari, M., Hassanzadeh, A., Khoshdast, H., 2024. Effect of different process water sources on rougher flotation efficiency of a copper ore: A case study at Sarcheshmeh Copper Complex (Iran). Physicochem. Probl. Miner. Process. Doi: 10.37190/ppmp/184087.

Sun, D., Li, M., Fu, Y., Pan, Z., Cui, R., Wang, D., Zhang, M., Yao, W., 2023. Selective Separation of Chalcopyrite from Pyrite Using Sodium Humate: Flotation Behavior and Adsorption Mechanism. ACS Omega 8, 45129–45136. Doi: 10.1021/acsomega.3c07539.

Unesi, M., Noaparast, M., Shafaei, S.Z., Jorjani, E., 2014. Modeling the effects of ore properties on water recovery in the thickening process. Int. J. Miner. Metall. Mater. 21, 851–861. https://doi.org/10.1007/s12613-014-0981-y.

Uribe, L., Gutierrez, L., Laskowski, J.S., Castro, S., 2017. Reverse flotation of ultrafine magnetic concentrate by using mixed anionic/cationic collectors. Physicochem. Probl. Miner. Process. ISSN 2084-4735 802 kB. Doi: 10.5277/PPMP170205.

Yang, Y., Kostović, M., Deng, R., Liao, Y., 2025. Study on the Inhibition and Activation of Pyrite under Low Alkalinity Conditions created by Hydrogen Peroxide and Lime. Minerals 15, 1177. https://doi.org/10.3390/min15111177.

Zanin, M., Lambert, H., Du Plessis, C.A., 2019. Lime use and functionality in sulphide mineral flotation: a review. Miner. Eng. 143, 105922. https://doi.org/10.1016/j.mineng.2019.105922.

Zhang, C., He, T., Chen, W., Bu, X., Wang, S., Tian, X., 2020. The Auxiliary effect of Copper Ions on the Depressant effect of Sodium Thioglycolate in Chalcopyrite Flotation. Minerals 10, 157. https://doi.org/10.3390/min10020157.

Zhang, C., Su, Y., He, T., Bu, X., Wan, H., Wang, S., Xue, J., 2025a. The role of copper ions in improving the flotation of chalcopyrite at low temperatures. Miner. Eng. 220, 109091. https://doi.org/10.1016/j.mineng.2024.109091.

Zhang, L., Li, A.-H., Jia, X.-X., Klemeš, J.J., Liu, Z.-Y., 2021. Design of total water networks of multiple properties based on operator potential concepts and an iterative procedure. Energy Environ. 32, 1130–1146. https://doi.org/10.1177/0958305X20919408.

Zhang, L., Liu, J., Ma, Z., Peng, W., Huang, Y., Wang, W., Cao, Y., 2025b. Recent advances in oxidation pretreatment and flotation separation of metal sulfide ores. Green Smart Min. Eng. 2, 142–155. https://doi.org/10.1016/j.gsme.2025.05.006.